

AIAA TEAM SPACE TRANSPORTATION  
DESIGN COMPETITION

---

**TEAM PERSEPHONE**

---



*Submitted By:*

Chelsea Dalton  
Ryan Decker  
Layne Droppers  
Zach Harmon  
Nicholas Malone

Ashley Miller  
Sahil Pathan  
Joshua Prentice  
Andrew Townsend  
Nicholas Wijaya

Iowa State University  
Department of Aerospace Engineering  
May 10, 2018

Iowa State University:  
Persephone Design Team



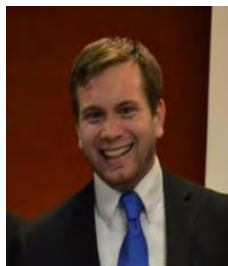
Chelsea Dalton  
Trajectory & Propulsion  
AIAA ID #908154

*Chelsea Dalton*



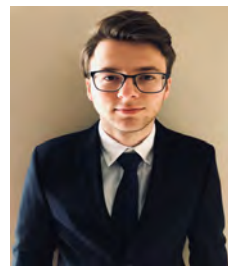
Ryan Decker  
Communications & Power  
AIAA ID #906791

*Ryan Decker*



Layne Droppers  
Team Lead  
AIAA ID #532184

*Layne Droppers*



Zachary Harmon  
Thermal Systems  
AIAA ID #921129

*Zachary Harmon*



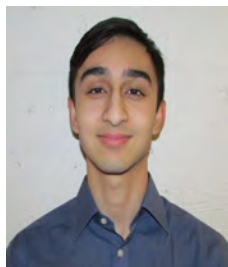
Nicholas Malone  
Orbit Design  
AIAA ID #921128

*Nicholas Malone*



Ashley Miller  
Science  
AIAA ID #922108

*Ashley Miller*



Sahil Pathan  
Science  
AIAA ID #761247

*Sahil Pathan*



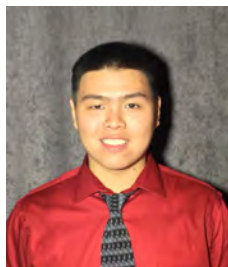
Joshua Prentice  
Science  
AIAA ID #922104

*Joshua Prentice*



Andrew Townsend  
Structures & CAD  
AIAA ID #820259

*Andrew Townsend*



Nicholas Wijaya  
Trajectory & Propulsion  
AIAA ID #644893

*Nicholas Wijaya*

## Contents

<b>1</b>	<b>Introduction &amp; Problem Background</b>	<b>2</b>
1.1	Motivation & Background . . . . .	2
1.2	Mission Definition . . . . .	3
<b>2</b>	<b>Mission Overview</b>	<b>5</b>
2.1	Trade Study Tools . . . . .	5
2.2	Mission Architecture . . . . .	6
2.3	Planetary Protection . . . . .	6
<b>3</b>	<b>Science</b>	<b>8</b>
3.1	Observations of Interest . . . . .	8
3.2	Goals . . . . .	9
3.3	Instrumentation . . . . .	10
3.3.1	Visible and Infrared Imaging—Ralph . . . . .	11
3.3.2	Radio Science Subsystem . . . . .	12
3.3.3	Atmosphere . . . . .	14
3.3.4	Solar Wind Around Pluto . . . . .	14
3.3.5	Descent Probes . . . . .	16
<b>4</b>	<b>Trajectory</b>	<b>19</b>
4.1	Interplanetary Trajectory Design . . . . .	19
4.2	Earth Launch . . . . .	19
4.2.1	Launch Vehicle Selection . . . . .	19
4.2.2	Launch Vehicle Integration . . . . .	22
4.2.3	Launch Characteristics . . . . .	23
4.3	Interplanetary Cruise . . . . .	25
4.4	Jupiter Gravity Assist . . . . .	26
4.5	Pluto Orbit Insertion . . . . .	28
<b>5</b>	<b>Primary Mission</b>	<b>30</b>
5.1	Design Methodology . . . . .	30
5.2	Phase 1: Pluto Observation . . . . .	30
5.3	Phase 2: Observation of the Moons of Pluto . . . . .	32
5.3.1	Charon . . . . .	32
5.3.2	Styx . . . . .	34
5.3.3	Nix . . . . .	34
5.3.4	Kerberos . . . . .	35
5.3.5	Hydra . . . . .	35
5.4	Phase 3: Pluto deorbit . . . . .	36
5.5	Secondary Mission Potential . . . . .	37
5.6	Spacecraft Disposal . . . . .	37

---

<b>6</b>	<b>Spacecraft Design</b>	<b>38</b>
6.1	Configuration & Overview . . . . .	38
6.2	Structure . . . . .	41
6.3	Propulsion . . . . .	42
6.3.1	Engine Type . . . . .	43
6.3.2	Engine Selection . . . . .	50
6.3.3	Propellant Selection . . . . .	52
6.4	Power . . . . .	53
6.4.1	Generation . . . . .	53
6.4.2	Batteries . . . . .	55
6.5	Command and Data Handling . . . . .	55
6.5.1	Main Computer . . . . .	56
6.5.2	Short & Medium-Term Storage . . . . .	56
6.5.3	Long-Term Storage . . . . .	57
6.6	Communications . . . . .	60
6.6.1	High Gain Antenna . . . . .	60
6.6.2	Medium Gain Antenna . . . . .	61
6.6.3	Low Gain Antennas . . . . .	61
6.6.4	Deorbit Reasoning and Calculations . . . . .	62
6.7	Thermal Control . . . . .	63
6.7.1	Passive Thermal Control . . . . .	63
6.7.2	Active Thermal Control . . . . .	64
6.7.3	Descent Probes Thermal Control . . . . .	65
6.8	Guidance, Navigation, and Control . . . . .	65
6.8.1	Overview . . . . .	65
6.8.2	Disturbance Torques . . . . .	66
6.8.3	System Selection . . . . .	67
6.9	Attitude Determination . . . . .	70
<b>7</b>	<b>Cost Evaluation</b>	<b>73</b>
<b>8</b>	<b>Mission Summary &amp; Conclusions</b>	<b>74</b>

## List of Figures

3.1	Ralph . . . . .	12
3.2	Cassini RSS . . . . .	14
3.3	SWAP Instrumentation . . . . .	15
3.4	NASA Standard Initiator . . . . .	17
3.5	descent probe . . . . .	18
4.1	SLS Launch Vehicle Configurations [14] . . . . .	22
4.2	Launch Vehicle Integration . . . . .	23
4.3	SLS C3 Performance . . . . .	24
4.4	Earth Launch . . . . .	24
4.5	Interplanetary Trajectory - Ecliptic Normal . . . . .	25
4.6	Interplanetary Trajectory - Ecliptic View . . . . .	26
4.7	B-Plane Definition [15] . . . . .	27
4.8	B-Plane Vector Components [15] . . . . .	27
4.9	Jupiter Gravity Assist . . . . .	28
4.10	Jupiter Gravity Assist - Ecliptic View . . . . .	28
4.11	Pluto Orbit Insertion . . . . .	29
5.1	First Month of Orbit . . . . .	31
5.2	Charon Observation . . . . .	33
5.3	Styx Observation (Styx in Blue) . . . . .	34
5.4	Nix Observation (Nix in Gray) . . . . .	34
5.5	Kerberos Observation (Kerberos in Lime Green) . . . . .	35
5.6	Hydra Observation (Hydra in yellow) . . . . .	35
5.7	Pluto deorbit . . . . .	36
6.1	Spacecraft Configuration—Front . . . . .	38
6.2	Spacecraft Configuration—Back . . . . .	38
6.3	Spacecraft Configuration—Forward . . . . .	38
6.4	Spacecraft Configuration—Aft . . . . .	38
6.5	Persephone Spacecraft Cutaway . . . . .	39
6.6	Titanium Frame . . . . .	42
6.7	Propulsion Systems Performance [18] . . . . .	43
6.8	Required Propellant Mass . . . . .	46
6.9	Required Maneuver Time . . . . .	47
6.10	Propellant Usage . . . . .	47
6.11	Solar Power Decay . . . . .	48
6.12	Plutonium Power Decay . . . . .	48
6.13	Hybrid Chemical Propellant vs. Arrival Velocity . . . . .	49
6.14	Hybrid NEP Capture Maneuver . . . . .	49
6.15	Hybrid NEP Propellant Usage . . . . .	49
6.16	Butek BHT-600 Engine . . . . .	52
6.17	Thruster Configuration . . . . .	52
6.18	GPHS-RTG Cutaway . . . . .	54
6.19	The DDC SCS750 computer . . . . .	56
6.20	The Solid State Recorder . . . . .	57
6.21	Integral 512GB MicroSD Card . . . . .	58

---

6.22	The 5-Module Redundant Data Storage Architecture . . . . .	59
6.23	High Gain Antenna . . . . .	61
6.24	Medium Gain Antenna . . . . .	61
6.25	Mission Disturbance Torque Breakdown . . . . .	67
6.26	Momentum Dumping during Mission . . . . .	69
6.27	Ball Aerospace CT-2020 Star Tracker [29] . . . . .	71
6.28	Adcole Fine Sun Sensor ( <i>courtesy Adcole Corporation</i> ) . . . . .	72
6.29	Bathtub Reliability Curve[30] . . . . .	72
8.1	Persephone Spacecraft . . . . .	74
8.2	Interplanetary Trajectory . . . . .	75

## List of Tables

1.1	Mission Requirements . . . . .	4
2.1	Planetary Protection . . . . .	6
3.1	Selected Scientific Instruments with Specifications . . . . .	11
4.1	Mission Scenarios to Pluto and KBO [2] . . . . .	20
4.2	Considered Launch Vehicles . . . . .	21
4.3	Criteria Weighting . . . . .	22
4.4	Vehicle Selection . . . . .	22
4.5	Launch Parameters . . . . .	24
4.6	JGA Parameters . . . . .	27
6.1	Spacecraft Mass Budget . . . . .	40
6.2	Mass Budget Summary . . . . .	41
6.3	SLS Payload Accelerations . . . . .	41
6.4	TRL Definitions . . . . .	42
6.5	Chemical & NTR Engine Comparison . . . . .	45
6.6	Electric Propulsion Engine Specifications . . . . .	46
6.7	Electric Engine Specifications . . . . .	51
6.8	Criteria Weighting . . . . .	51
6.9	Engine Selection . . . . .	51
6.10	Tank Optimization Weightings . . . . .	52
6.11	Propellant Tank Optimization . . . . .	53
6.12	RTG Comparison . . . . .	54
6.13	DDC SCS750 Specs . . . . .	56
6.14	MicroSD Specifications . . . . .	58
6.15	Data Rates During Return to Earth . . . . .	62
6.16	Maximum Disturbance Torques . . . . .	66
6.17	Mechanical vs. Magnetic Bearing Reaction Wheels . . . . .	68
6.18	Hydrazine Tank Design . . . . .	70
7.1	Mission Cost Analysis . . . . .	73
8.1	Mission Timeline . . . . .	74

## Nomenclature

AHP	Analytical Hierarchy Process
BFR	Big Falcon Rocket
BOL	Beginning of Life
C3	Characteristic Energy
CCHP	Constant Conductance Heat Pipe
DS1	Deep Space 1
DTR	Digital Tape Recorder
EOL	End of Life
GCMS	Gas Chromatography Mass Spectrometry
GPHS	General Purpose Heat Source
IMU	Inertial Measurement Unit
ISP	Specific Impulse
JGA	Jupiter Gravity Assist
JPL	Jet Propulsion Laboratory
LEISA	Linear Etalon Imaging Spectral Array
MLB	Motorized Light Band
MLI	Multi-Layer Insulation
MMRTG	Multi-Mission Radiothermal Generator
MPG	Mission Planner's Guide
MVIC	Multispectral Visible Imaging Component
NEP	Nuclear Electric Propulsion
NERVA	Nuclear Engine for Rocket Vehicle Application
NSI	NASA Standard Initiator
NTR	Nuclear Thermal Rocket
PKB	Pluto-Kuiper Belt
POI	Pluto Orbit Insertion
RCS	Reaction Control System
REX	Radio Science Experiment
RFP	Request for Proposal
RSS	Radio Science Subsystem
RTG	Radioisotope Thermoelectric Generator
RWA	Reaction Wheel Assembly
SEP	Solar Electric Propulsion
SLS	Space Launch System
SNAP	System for Nuclear Auxiliary Power
SOA	State of the Art
STK	Satellite Tool Kit
SWAP	Solar Wind Around Pluto
TCM	Trajectory Correction Maneuver
TRL	Technology Readiness Level
TWTA	Traveling Wave Tube Amplifier



# 1 Introduction & Problem Background

## 1.1 Motivation & Background

The Persephone mission will investigate the Pluto-Charon system and attempt to answer the many questions left unanswered after the first visit by New Horizons. The mission will use advanced instrumentation to image and analyze the geology, atmosphere, and surface composition of the Pluto-Charon system.

Interest in a Pluto mission dates back to the 1990s, where a postage stamp sparked the interest of employees at NASA's Jet Propulsion Laboratory (JPL) [1]. Pluto received many mission proposals over the following years, yet none found much traction until NASA began soliciting proposals for the Pluto-Kuiper Belt (PKB) mission in 2001 [2]. Later that same year, NASA officially selected the New Horizons proposal to be the first mission to visit the icy outer planet. By 2006, New Horizons had launched on a trajectory to Pluto. Using a Jupiter Gravity Assist (JGA), the probe arrived at Pluto nine and a half years later and revealed to the scientific community a completely unexpected world.

Long thought to be a dead relic left over from the formation of the solar system, New Horizons instead revealed Pluto to be a dynamic, changing world. Its geology ranges extensively from large, uncratered plains to rugged mountains. Pluto shows fault trends that suggest a long history of prolonged tectonic activity. In contrast, Sputnik Planum, a young plain estimated to be less than 10 million years old, shows evidence of volatile ices going through convection and advection [3]. Between ancient features that detail Pluto's history and young plains that hint at its recent past, the geology uncovered by New Horizons shows a complex history for the ancient dwarf planet. Signs of dynamic landscape remodeling implore further investigation.

Additionally, Charon displays complex geology, with a heavily cratered northern hemisphere and a younger, smoother southern hemisphere. While its many features fit into the general model of icy satellites as they age, the evolutionary history of Charon is still quite uncertain. Questions remain regarding Charon's geologic history and how its surface has maintained a current level of geographic complexity [3].

New Horizons also succeeded in characterizing and profiling Pluto's atmosphere. While it helped to confirm many predicted models, and there were many surprises that were uncovered as well. Most notably,

it was discovered that Pluto's atmospheric nitrogen escape is happening at a rate that is roughly 10,000 times slower than what was originally predicted [4], and the interaction of Pluto's atmosphere with Charon is still not quite understood. Some of the data gathered by New Horizons shows evidence of Pluto's atmosphere leading to tholins being accumulated on Charon's northern hemisphere, leaving a dark-red northern pole [5]. This phenomenon could use additional long-term observation, especially as Pluto progresses through its seasons.

The first glimpses of Pluto's smallest satellites—Styx, Nix, Kerberos, and Hydra—were provided by New Horizons. Basic imaging allowed for the primary categorization of the satellites, including their size, albedo, and rotational and revolutionary periods. These observations hint at a water-ice surface composition of all satellites with a common formation age of at least four billion years ago. Initial observations also provide substance to the giant collision theory of this system's formation [6]. While this data gives a great first picture of the system, there is still much to learn from the system's smaller satellites.

While New Horizons officially introduced the Pluto-Charon system to the world in 2015, the data it collected during its brief flyby only scratched the surface of the science behind its geology, atmosphere, and history. Persephone is designed to follow the science that has been conducted by New Horizons and to answer the lingering questions left behind from initial observations. Persephone also aims to study Pluto as it moves further from the Sun, hoping to capture some of the dynamic processes that occur throughout Pluto's year.

## 1.2 Mission Definition

This proposal is written to answer the Request for Proposal (RFP) put forth in the 2017-2018 AIAA Undergraduate Team Space Transportation Design Competition. The AIAA RFP contains broad requirements for an orbital mission to Pluto using current or near-current propulsion technology with many of the same mass and instrumentation constraints as New Horizons. The high-level requirements of the Persephone mission are illustrated in Table 1.1.

Table 1.1: Mission Requirements

<b>Requirement Number</b>	<b>RFP Para. Number</b>	<b>Description</b>
1	1	The primary mission length shall be less than 25 years.
2	1	A minimum of one year shall be reserved for the Pluto orbital mission.
3	1	The in-space propulsion system shall have a TRL of 6 or higher.
4	1	The base instrumentation load shall be based on New Horizons.
5	2	The dry mass of the spacecraft shall be no more than that of New Horizons.
6	4	The mission architecture shall be constrained to a single launch vehicle.

## 2 Mission Overview

Persephone is a spacecraft designed to follow in the footsteps of New Horizons as a Pluto orbiter. This is a unique problem for two key reasons. The first is that no spacecraft has ever captured into orbit around an object so far from the Sun. While this may seem trivial at first, the distance from the Sun has a significant impact on the mission design. In order for a mission to reach Pluto in a reasonable amount of time, the probe must be on a hyperbolic trajectory out of the solar system; however, using a hyperbolic trajectory to get to Pluto creates an immense amount of kinetic energy. If an orbital mission is desired, then this kinetic energy must be nearly entirely eliminated in order to capture around the dwarf planet. Thus, this mission is an inherent balance between mission time and the energy required to capture into orbit.

The second key reason is that while other spacecraft have captured around planets in the outer solar system before, those spacecraft have had the advantage of an enormous gravity-well at their disposal. Capturing into an orbit around a gas giant is easier than capturing around a dwarf planet with a mass one-sixth of the moon. Coupling this problem with the previous one, it is evident that there is an enormous strain placed on the spacecraft propulsion system. This mission design takes various approaches in order to accomplish the mission objectives.

The Persephone mission will utilize a combination of gravity assists and advanced propulsion methods to accomplish the 25-year mission.

### 2.1 Trade Study Tools

For many of the broad mission decisions, the analytical hierarchy process (AHP) is used. This tool is a powerful, decision-making method which aids in minimizing inherent biases. By using pairwise comparisons between specific evaluation criteria and a set of alternative options, relative weightings are given to each alternative which allow mission designers to more easily assess how well a given alternative meets the requirements. AHP captures both subjective and objective evaluation measures, providing a useful mechanism for checking the consistency of the evaluation measures and alternatives suggested [7]. Utilizing AHP for primary, high-level decisions allows for quick decision making and rapid development of

the Persephone mission concept.

When AHP is not sufficient, system optimization techniques and cost functions are used to evaluate potential alternatives and determine the best option. These techniques are particularly useful when it comes to spacecraft subsystem design where an engineering approach is best suited to find the optimal solution.

## 2.2 Mission Architecture

The mission architecture is broken into three primary categories: Earth launch, interplanetary cruise, and Pluto orbital mission. Each of these categories encompass numerous key decisions that together comprise the Persephone mission. Additional consideration is given to a fourth category, secondary mission potential, but it is not a major factor in the mission architecture chosen due to its omission from the RFP. Each of these categories require a thorough analysis through trade studies and optimization and will be discussed in detail later on in this proposal.

## 2.3 Planetary Protection

NASA's Office of Planetary Protection requires that every mission to a planetary body must meet certain cleanliness standards based on the target body and the type of mission—flyby, orbiter, or lander. According to NASA guidelines, Persephone is classified as a Category II mission because Pluto is of significant interest relative to the process of chemical evolution but only a remote chance that contamination by spacecraft could compromise future investigations [8]. Further definition of this protection category is given in Table 2.1.

Table 2.1: Planetary Protection

Category II	Flyby, Orbiter, and Lander	Icy satellites, where there is a remote potential for contamination of the liquid-water environments, such as Ganymede (Jupiter); Titan (Saturn); Triton, Pluto and Charon (Neptune); others TBD.
-------------	----------------------------	---

This categorization does not place any restrictions on mission operations but only requires that proper documentation be provided. This documentation includes a Planetary Protection Plan, a Pre-Launch Planetary Protection Report, a Post-Launch Planetary Protection Report, and an End-of-Mission Report. These reports will address impact avoidance strategies and the actual disposition of the spacecraft upon mission conclusion [8].

## 3 Science

### 3.1 Observations of Interest

New Horizons launched in January 19, 2006 as a part of the New Frontiers Program to research Pluto. In 2015, New Horizons conducted scientific observations during its Pluto flyby. In the brief period in which New Horizons monitored Pluto, the probe made many significant observations.

Perhaps the most significant discovery was Sputnik Planum, a young, massive ice glacier—approximately 10 million years old—with no detectable craters. This feature and additional dating of Pluto’s surface revealed a geologically active Pluto that has been dynamically changing over the past four billion years. The unexpected discovery of complex nitrogen, methane, and water further hinted at Pluto’s volatile geologic history, with distributions of these elements not found anywhere else in the solar system.

New Horizons found the upper atmosphere temperature to be much colder than expected. This phenomenon significantly affects the atmospheric escape rate, which was also found to be much lower than anticipated. Categorization of Pluto’s atmosphere revealed the atmospheric composition as a function of altitude and showed varying amounts of molecular nitrogen, methane, acetylene, ethylene, and ethane. Atmospheric haze layers were discovered to be formed by the atmospheric buoyancy waves created by winds blowing over the mountainous surface.

The particle density around Pluto was measured to be not much higher than typical vacuum conditions at six particles per cubic mile. This measurement shows a relatively debris-free Pluto, and provides some context on the behavior Pluto’s interactions with its moons.

New Horizons observed interactions with the solar wind around Pluto at an altitude of seven thousand kilometers and found a much lower interaction rate than what was expected. This discovery can partially be linked to the lower atmospheric escape rate measured. However, further research must be conducted to obtain a deeper understanding of the system’s atmosphere and the gaseous release process it experiences.

A reflectivity of 50 to 80 percent was measured for all of Pluto’s satellites. These reflectivities are much higher than what has been observed for most Kuiper Belt objects, which are around 5 to 20 percent reflective. This abnormality suggests the possibility of an ancient collision, which resulted in the formation

of Pluto's satellites from the remnants of the dwarf planet itself.

Using these discoveries as reference, the scientific priorities of the Persephone mission are determined via an AHP analysis. The analysis focuses on furthering the scientific discoveries made by New Horizons as well as new observations that the scientific community desires. Observation options are against one other based on feasibility, scientific discovery potential, and probability of success. From this analysis, the most meaningful scientific observations for the mission include detailed imaging in the visual and infrared spectrum of all bodies in the Pluto System, analyzing the shared atmosphere of Pluto and Charon, studying the topography of the celestial bodies, and observing interactions of the system with the solar wind.

### 3.2 Goals

The scientific goals are determined based on the observations of interest and the scientific instruments that were feasible. The majority of the scientific instruments chosen are intended to study the subsurface composition and possible geologic activity of Pluto, specifically around the edges of Sputnik Planum. Utilizing a series of low orbits, the active Sputnik Planum region will be further studied. Furthermore scientific instruments will be chosen to attempt to find the source of geological activity. It is suspected that there are cryovolcanoes in the Sputnik Planum region. The descent probes will gather information that will show what the cryovolcanoes look like and what their surface temperatures are. Persephone will determine the density of the material on the surface and underneath the surface. The surface of Pluto is comprised of a mixture of nitrogen, methane, and water. The geological activity may have changed the temperature, concentration, or phase of the materials found on and below the surface.

The other main goal of this mission is to study the atmosphere of Pluto over a larger period of time than New Horizons was capable of, specifically the escape rate of the atmosphere to Charon and space as well its interactions with the solar wind. This interaction is thought to be the source of low energy x-rays coming from Pluto but was not closely observed by New Horizons for a long period of time.

While in orbit, Persephone will be able to map the previously unmapped and unobserved portions of Pluto and Charon. Persephone will capture in higher resolution areas that were previously imaged. Persephone's imaging wavelength range will determine more information for analysis regarding the history



of the surfaces of Pluto and Charon. Determining the composition and capturing a detailed image of those surfaces will provide insight for understanding the history of these surfaces.

Finally, this mission hopes to provide better data and insight on the moons of Pluto (mainly Charon). Persephone will capture images and receive radiowave data. This information will be used to map in higher resolution both Charon's surface and the surfaces of Pluto's other moons. Persephone will capture information about the interaction of escaping gas particles with Pluto and Charon and determine if any similar effect is on the other moons. Persephone will capture information about the materials through density analysis on every body within passing orbit. Thermal information will also be captured and will be used to determine, along with visible light spectrum imaging information, the reason for the high reflectiveness of Pluto's satellites. It is projected that one of the three descent probe probes will be launched onto Charon to capture visual and thermal information. Analysis of this information will allow for the understanding of the origin of the satellites, their surface properties, and any geological surface activity,

### **3.3 Instrumentation**

New Horizons was equipped with seven different scientific instruments. Each instrument was fixed within the structure of the spacecraft. New Horizons needed to orient the spacecraft to point a scientific instrument at a specified location. New Horizons was capable of optical imaging, infrared and ultraviolet spectroscopy, and particle and dust sensing.

Persephone will capture similar capability to New Horizons being capable of optical imaging and infrared spectroscopy. Persephone will use its scientific instruments to focus on specific areas of interest within Pluto. Persephone will use the same instruments as New Horizons in imaging and spectroscopy, and it will add a radio science subsystem. It is assumed all instruments will have increased efficiency and effectiveness based on a certain amount of time passing since its initial creation. All instruments will use modified values for power consumption weight and resolution (for imagers).

Table 3.1: Selected Scientific Instruments with Specifications

	<b>Instrument</b>	<b>Mass (kg)</b>	<b>Power (W)</b>
<b>Visible and Infrared Imaging</b>	Ralph	33	50(nominal) 70(peak)
<b>Solar Wind</b>	SWAP	3.30	2.3
<b>Radio Science</b>	RSS	0.1	2.1
<b>Atmosphere</b>	CAPS	19.5	41

### 3.3.1 Visible and Infrared Imaging—Ralph

Persephone will use an infrared/visible imager to find geothermally active locations near the Sputnik Planum. It will use an upgrade from New Horizons' Ralph instrument. There are alternatives to Ralph such as Virtis from ESAs Rosetta mission; however, Ralph has the imaging capability and thermal sensitivity to observe the missions areas of interest. Ralph is comprised of two subinstruments: MVIC and LEISA.

Multispectral Visible Imaging Component (MVIC) is a visible imager capable of covering four bands in the visible light spectrum. MVIC is able to provide color images of Pluto and Charon at a resolution up to one kilometer per pixel. Ralph's primary objective was to map the basic geography of Pluto and search for unique features such as rings or additional moons. Persephone will repurpose Ralph to develop detailed imagery of key locations.

Linear Etalon Imaging Spectral Array (LEISA) is capable of mapping certain materials on the sunlit surface and mapping surface temperatures. LEISA is capable of roughly mapping areas differing between chemical compositions such as water, methane, carbon dioxide, nitrogen ice, and other materials.

Together, MVIC and LEISA provide a method to deliver full color images of Pluto. Previously pixelated images of Pluto were replaced by Ralph's full color imagery. Persephone will use an upgraded version of Ralph with lower power consumption and higher resolution. The new and repurposed Ralph will be focused on completing a higher resolution capture of Pluto and Charon. Ralph will capture clear and close images of areas of interest, such as the Sputnik Planum. Ralph will capture images of unique features pertaining to crevices and possible cryovolcanoes to further the understanding of the Sputnik Planum

region. A higher resolution Ralph will capture the clearest images of Pluto and Charon to date as well as fully map the surface of Pluto. Following the imaging of Pluto, Persephone will use Ralph to capture visual information on Charon and Pluto's other moons. Ralph can be seen below in Figure 3.1.

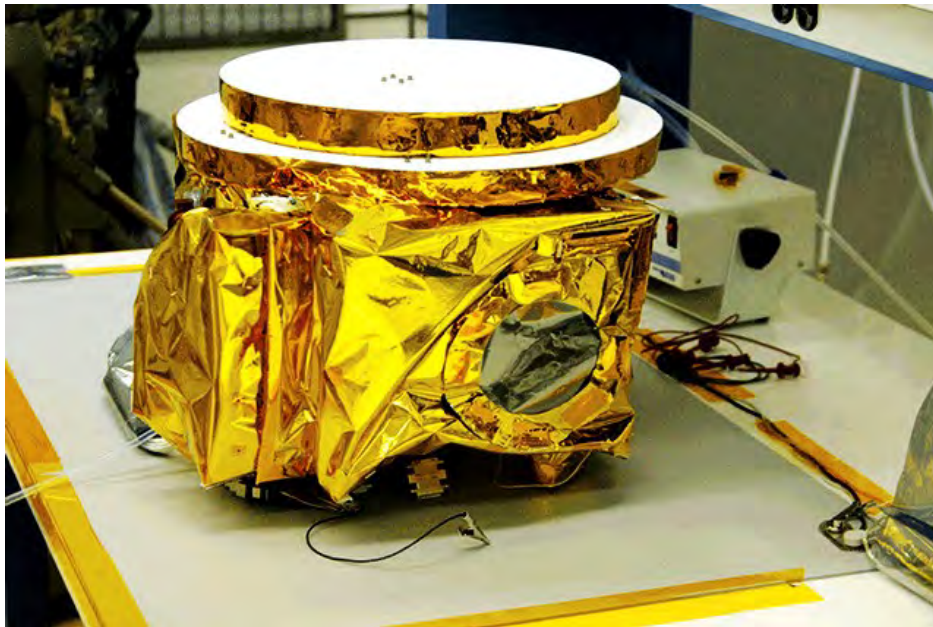


Figure 3.1: Ralph

### 3.3.2 Radio Science Subsystem

This instrument is taken from the Cassini Radio Science Subsystem (RSS) that was used to observe the Doppler shift in radio waves sent from the satellite [9]. This instrument will repeat the RSSs process, but will observe the Doppler effect due to Pluto and the surrounding bodies. This does not rely on data rate, but only relies on the Doppler shift of the received signal and is independent of its contents. Data from this observation can be collected on a variety of subjects.

The RSS can operate in the Ka, S, and X band frequencies and requires little mass or power as it mostly utilizes a high gain antennae when sending data back to Earth; however, one critical part of the RSS is on Earth. The RSS will require the coordination of the Deep Space Networks in Spain, Australia, and in the United States, which are the same networks that the Cassini RSS used. The benefit of these

networks is that all of the RSS results will be available in real time as the signal is received on Earth. The transmission itself is the experiment [9].

To see what parts of the Pluto system the RSS can study, the Cassini mission provides several useful precedents: the signal can be sent through the atmosphere of Pluto or Charon, and the signal will bend due to the density of the atmosphere. The density is then dependent on the temperature and pressure of the atmosphere yielding further information about Pluto's atmosphere than New Horizons and over a much longer period of time. It should be noted that Cassini used this method to measure properties of Titan's very thick atmosphere, so there is a concern with the sensitivity when studying Pluto's or Charon's atmospheres; however, the RSS of Cassini was said to have the ability to detect a sheet of paper between Saturn and Earth indicating it was a highly sensitive instrument [10]. The RSS was repeatedly used to eventually describe the entire structure of Saturn's atmosphere. The RSS was also used to measure the size of particles in Saturn's rings as well as the rings' structures. Though the Pluto system does not have any rings, there is a flow of particles from Pluto to Charon due to the solar wind hitting Pluto. The RSS on Persephone could at least find the density of these particles and the structure of the transiting particles. As with all the observations by Persephone, this "stealing" of the atmosphere can be observed over years rather than over a matter of hours as with New Horizons. One potential discovery is to see if there is a subsurface ocean on Pluto underneath one of the glaciers. There is reason to believe an ocean is possible given the evidence of new geologic activity and a significant amount of water ice. The RSS instrument will be able to detect any subsurface liquid bodies by observing the Doppler shift due to the gravitational field of Pluto. This shift will be different if any significant portion of Pluto consists of a liquid rather than a solid, which was also done during the Cassini mission and led to the conclusion that Titan and Enceladus both likely have deep subsurface liquid water oceans [10]. The Cassini RSS is shown in Figure 3.2.



Figure 3.2: Cassini RSS

### 3.3.3 Atmosphere

Persephone will use an ion and neutral mass spectrometer to study the atmosphere of Pluto and Charon. This instrument is used to determine the composition and structure of positive ions and neutral particles in the upper atmospheres of Pluto and Charon. The instrument will also measure the flux of particles through the detector to determine the escape rate of the atmosphere. During the mission, Pluto will have a northern summer and southern winter. The instrument will observe the atmospheric changes as the CH<sub>4</sub>, N<sub>2</sub>, and CO ice present on Pluto's surface evaporate.

### 3.3.4 Solar Wind Around Pluto

Pluto has a comet-like phenomenon occurring regarding its atmosphere. It is slowly losing particles of its atmosphere due to the supersonic solar wind. As Pluto continues its orbit, it leaves a trail of these particles that tend to gravitate toward Charon; however, this interaction changes as Pluto gets further from the sun. The escape rate of the particles slows and Pluto's atmosphere contracts and freezes on the

surface due to the cold temperatures. This freezing creates a layer of N<sub>2</sub> estimated between 0.5 and 3 km thick, which could significantly affect Pluto's topography and potentially explain the geologically young surface in some locations such as Sputnik Planum. New Horizons was able to use the Solar Wind Around Pluto (SWAP) instrument while Pluto was closer to its perihelion, and the escape rate was nonzero. The Persephone mission will reuse this instrument and given the mission timeline, it will be observing Pluto as it continues to head towards its aphelion. This means the escape rate will be slowing down due to the cooling. Because Persephone is an orbiter, the escape rate will be observed for multiple years, and a gradual slowing of atmosphere loss will be observed in addition to the escape rate and the deceleration of that rate estimated [11].

X-rays have been confirmed to be emanating from Pluto via x-ray telescopes on satellites orbiting Earth. These are suspected to be the result of solar wind interacting with the minimal atmosphere of Pluto causing it to slowly escape as well as possibly emit low energy x-rays. It would be valuable to repeat the use of the SWAP instrument that New Horizons used in order to get prolonged data on the solar wind, the interactions, and possibly the resulting x-rays. This data combined with observations from x-ray telescopes orbiting Earth could provide more insight into why the x-rays are created. SWAP will also assist the GCMS in determining the escape rate of the atmosphere from Pluto over time to observe highs and lows of that transmission. At 3.3 kilograms and drawing 2.3 Watts, SWAP is an ideal instrument for this application [12], and is shown in Figure 3.3.



Figure 3.3: SWAP Instrumentation

### 3.3.5 Descent Probes

For this mission, Persephone will carry three detachable probes. The probes will record information during descent and ultimately crash into Pluto's surface. The probes are in the shape of cones with a diameter of 0.51 meters, a height of 0.61 meters, and a volume of 0.165 cubic meters. Each probe is point-heavy and will have four small fins to assist with the aerodynamic stability during descent, with the overall weight at 5 kilograms per probe. Each probe will contain a suite of scientific instruments: a visual spectrum imager, a thermal imager are the two primary instruments, but the probes will also carry small temperature, light, and pressure sensors. The two imagers are best suited to take more detailed images of Pluto as the probe descends through the atmosphere. All the components are powered by a lithium battery contained in the center of the probe. Each probe contains two small processors, one for redundancy. The STM32L4 microprocessor was chosen as the baseline for the probes. During the trip to Pluto, the probes will be heated to a minimum of  $-40^{\circ}\text{C}$  using resistor heaters, although the nominal temperature will be closer to the internal temperature of the main body. In orbit of Pluto, the descent probe probes will charge their batteries and be fed initial position information. The probe will then detach from the spacecraft using four NASA Standard Initiator (NSI), as shown in Figure 3.4. The four NSIs provide each probe with  $\sim 120$  m/s  $\Delta V$ ; enough to lower the periapsis into the surface of Pluto. It is not intended for the probe to land exactly on the targeted region of Sputnik Planum. The initial position is used to calculate the desired detachment time. The probes will not require active attitude control due to the thin atmosphere, the aerodynamically stable design, and the tolerance for landing location.



Figure 3.4: NASA Standard Initiator

The probes are intended to collect information as they descend toward the Sputnik Planum region. The probes will be contained in three separate containers which will be opened using a spring mechanism prior to detachment. The probes will be detached while in orbit of Pluto, pointing retrograde to the orbit of the main spacecraft.

Out of the possible areas of interest, it is planned to drop two descent probes onto the Sputnik Planum region. Sputnik Planum is of interest due to speculation of having a subsurface ocean and possibility of cryovolcanism. The landers are not intended to survive impact on the surface. The intent is to send two of the probes to Pluto, and if possible, to send one to Charon in order to gather similar information about Pluto's moon. The third probe will act as a redundant measure and will be sent to Pluto instead if either of the first two probes fail. The first probe will descend toward the western edge of the Sputnik Planum region followed by the second probe shortly after. The second probe will be sent toward the eastern edge of Sputnik Planum. If one or both of the probes fail, the third probe will be directed toward either the western or eastern edge of Sputnik Planum. If the first two probes do not fail, the third probe will be directed at Charon's northern pole.

The mothership is capable of observing visible and infrared spectrums. As opposed to the mothership, the probes' primary objectives are more centralized to the region of interest. The thermal camera will measure thermal activity nearing areas of suspected high geological activity. Probe placement near the edge of Sputnik Planum will ensure that the probes will be near areas suspected of geological



activity. The probes will relay thermal information in order to identify possible cryovolcanoes and confirm if any ridges or crevices near the perimeter of Sputnik Planum are geologically active. These probes will be able to record images in visible and thermal spectrums with relative quality of resolution from the fins that stabilize the probes in descent. In order to get high resolution images, the descent probes will be enter Pluto's thin atmosphere at a low angle. The other sensors included on the probes will record and measure conditions within the atmosphere as each of the probes descend. The descent will not generate enough heat, due to the atmospheric density, to damage the probe. The temperature of the probe will cool faster than it will heat up from entry into Pluto's atmosphere.

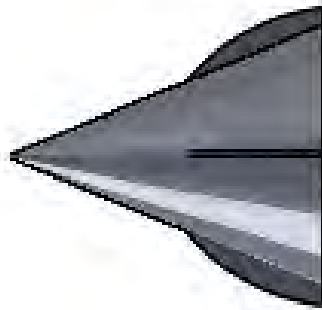


Figure 3.5: descent probe

## 4 Trajectory

### 4.1 Interplanetary Trajectory Design

Spacecraft trajectory optimization is important to the overall mission success. The trajectory design for this mission is a fine balance between the Pluto-Charon arrival time and the amount of fuel required. The proper balance between mission duration and fuel consumption must be determined. To minimize the arrival time, all avenues of trajectory design are examined—including single gravity assists from the gas giants, multiple gravity assist missions, and various propulsion methods. Launch window flexibility also plays an important role.

Various optimization tools were considered when developing the mission trajectory. Initial design considerations began with the use of an open-source Lambert solver which supported multiple gravity assist interplanetary trajectories [13]. This tool allowed a wide variety of complicated flight paths to be quickly considered with relative ease. The use of this tool enabled more promising trajectories to be analyzed with Satellite Tool Kit (STK), a higher-fidelity astrodynamics software. The use of this tool demonstrates the ease at which trajectories can be determined with relatively high fidelity. Orbital disturbances such as solar radiation pressure and multiple bodies are taken into account, which allows for a highly reliable trajectory to be designed.

### 4.2 Earth Launch

#### 4.2.1 Launch Vehicle Selection

An interplanetary mission to Pluto requires a significant amount of characteristic energy (C3) for reasonable mission duration. The utilization of all available energy resources is critical to reducing strain on the spacecraft design. C3 reduction techniques include utilizing larger launch vehicles and planetary gravity assists. Otherwise, the remaining C3 energy must come from the spacecraft propulsion system.

To better understand this problem, previous Pluto mission analysis is referred to. For the New Horizons mission design, an extensive analysis of potential launch windows was conducted by John Hopkins and can be seen in Table 4.1. This table displays the high C3 energies needed, the narrow launch windows, the complicated trajectory designs, and the wide range of possible mission durations.

Table 4.1: Mission Scenarios to Pluto and KBO [2]

Mission scenario	Launch		Encounter	
	Period	C3 (km <sup>2</sup> /s <sup>2</sup> )	Body	Year
2006 Baseline JGA or Pluto-direct → Pluto → KBOs	35 days (January 11–February 14)	164	Pluto	2015– 2020
2007 Backup Pluto-direct → Pluto → KBOs	14 days (February 2–15)	166.2	Pluto	2019– 2020
2006 Launch JGA → Pluto → KBOs	20 days (January 10–29)	166	Pluto	2015
	20 days (January 9–28)	156.7	Pluto	2016
2006 Launch (extended launch period) Pluto-direct → Pluto → KBOs	16 days (January 30–February 14)	166	Pluto	2019
	4 days (February 5–8)	156.7	Pluto	2020
2006 Launch 2+ year $\Delta V$ EGA → Pluto → KBOs	20 days (January 7–26)	28.2	Pluto	2015
	20 days (January 3–22)	28.4	Pluto	2016
	20 days (December 24–January 13)	28.8	Pluto	2020
2006 Launch 3+ year $\Delta V$ EGA → Pluto → KBOs	20 days (January 18–February 6)	50.4	Pluto	2015
	20 days (January 13–February 1)	50.6	Pluto	2016
	20 days (January 4–23)	51	Pluto	2020
2006 Launch 4+ year $\Delta V$ EGA → Pluto → KBOs	20 days (January 27–February 15)	65.1	Pluto	2015
	20 days (January 22–February 10)	65.3	Pluto	2016
	20 days (January 10–29)	65.8	Pluto	2020
2007 Launch Pluto-direct → Pluto → KBOs	10 days (February 4–13)	165	Pluto	2019
	10 days (February 4–13)	162.3	Pluto	2020
2008 Launch Pluto-direct → Pluto & KBOs	10 days (February 7–16)	168.5	Pluto	2020
2008 Launch JGA → Neptune → KBOs	20 days (March 15–April 3)	161	Neptune	2018
2008 Launch JGA → Uranus → KBOs	20 days (March 9–28)	109	Uranus	2015
2008 Launch JGA → KBO (1992 QB1)	20 days (March 8–27)	99	1992 QB1	2025
2009 Launch SGA → Pluto → KBOs	20 days (November 18–December 7)	148	Pluto	2022
2010 Launch SGA → Pluto → KBOs	20 days (November 30–December 19)	143	Pluto	2024

Notes: JGA, Jupiter gravity assist; SGA, Saturn gravity assist; 2+, 3+, 4+ year  $\Delta V$  EGA, deep space burn-Earth gravity-assist trajectory with time of flight more than 2, 3, or 4 years of the Earth return orbit

From the analysis of previous mission architectures, it is quite evident that the sensitivity to the launch date and launch C3 is paramount to mission viability and success; therefore, this mission design places a strong focus on innovative trajectories and high performance launch vehicles.

Presently, there are only a few launch vehicles capable of providing the spacecraft with high enough C3 to actually achieve the mission goals; however, a number of heavy-lift launch vehicles are currently under development by NASA and other commercial groups, many of which plan on flying by the mid-2020s. These developmental launch vehicles are included for consideration in the mission design while factoring into account the potential options with significant consideration given to realistic availability of the vehicle by the desired launch window. The considered launch vehicles are listed in Table 4.2.

Table 4.2: Considered Launch Vehicles

Ariane 5
Ariane 6
Atlas V
Big Falcon Rocket (BFR)
Delta IV Heavy
Falcon 9
Falcon Heavy
New Glenn
Space Launch System (SLS)
Vulcan

Presently, six of the 10 considered launch vehicles are under development with initial launch targets within the next five years. Using the AHP process, the criteria weightings and the resulting final weightings are shown in Tables 4.3 and 4.4, respectively.

Table 4.3: Criteria Weighting

Metric	Weight
Availability	0.4921
Reliability	0.2172
C3 Energy	0.1332
Cost	0.0785
TRL	0.0509
Scheduling	
Reliability	0.0280

Table 4.4: Vehicle Selection

	Weight
SLS	0.2934
Falcon Heavy	0.2306
Atlas V	0.1860
BFR	0.1498
Falcon 9	0.1401

During the selection process, it was determined that the operational readiness (availability), launch energy, and reliability of the rocket were the most critical criteria for this mission; therefore, NASA’s SLS was selected since will aid in providing the shortest transit time with a high probability of success.

#### 4.2.2 Launch Vehicle Integration

Ensuring that the spacecraft can integrate with the selected vehicle is very important. The SLS has multiple launch configurations, and these configurations include various performance characteristics and size requirements for the spacecraft as shown in Figure 4.1.

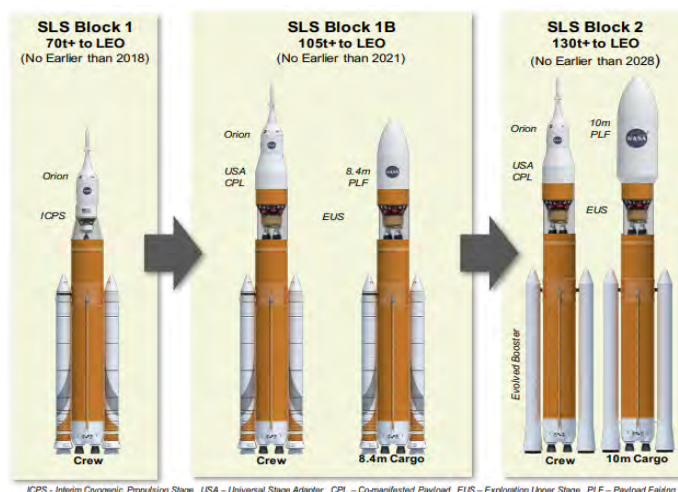


Figure 4.1: SLS Launch Vehicle Configurations [14]

Based on availability and performance requirements, Persephone will launch upon an SLS Block 1B Cargo configuration. Payload integration with the fairing is critical. Because volume is not a major concern for this spacecraft mission, the SLS 8.4 m short payload fairing concept will be utilized. Integrating the spacecraft with a payload attach fitting, a payload interface adapter, and a payload separation system, will ready it to be launched on the SLS. The final launch configuration can be seen in Figure 4.2.



Figure 4.2: Launch Vehicle Integration

### 4.2.3 Launch Characteristics

Using NASA's SLS Mission Planner's Guide (MPG), the performance of the launch vehicle can be determined given the payload mass provided. The available C3 energy, available as a function of payload mass, is shown in Figure 4.3. With a spacecraft mass of 1,200 kg, the location of this mission is shown from the red lines.

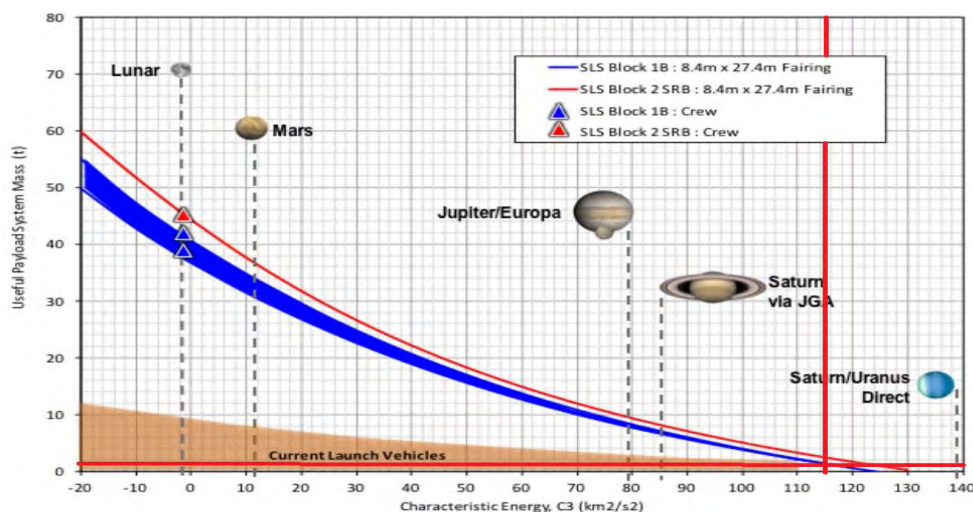


Figure 4.3: SLS C3 Performance

Given this payload mass, the SLS is able to provide a maximum  $C3$  of  $115 \text{ km}^2/\text{s}^2$ . While the trajectory does not have to use all of the  $C3$  energy, any unused amount is essentially wasted. This high  $C3$  energy allows for a more broad trajectory search, thus providing more potential trajectory solutions for this mission profile.

Utilizing STK, the nominal launch trajectory utilizes the entirety of the available  $C3$  energy to decrease mission's duration. The chosen launch parameters can be seen in Table 4.5, and the STK launch model can be seen in Figure 4.4.

Table 4.5: Launch Parameters

Launch Date	7 Jan 2030
C3	$115 \text{ km}^2/\text{s}^2$
RA	$217.62^\circ$
DEC	$-10.59^\circ$



Figure 4.4: Earth Launch

### 4.3 Interplanetary Cruise

After launch, the spacecraft begins its interplanetary cruise phase. This cruise phase is the primary mode of the spacecraft for the majority of its mission. During this time, nearly all systems are dormant and only wake up periodically to ensure nominal operation. The spacecraft will be spin-stabilized to minimize the need for attitude control intervention. Throughout this cruise phase, it is expected that a few trajectory correction maneuvers (TCMs) will need to be performed.

The cruise phase is broken down into two main segments, which are separated by a Jupiter Gravity Assist (JGA). The first segment occurs from Earth to the JGA and takes one year, five months, and three weeks. The second segment takes longer and occurs from JGA to the deceleration for Pluto orbital insertion (POI) phase. This second phase takes an additional 12 years. In total, the spacecraft spends nearly the first 13.5 years of its mission on an interplanetary coast trajectory. The perspectives of this trajectory are shown in Figures 4.5 and 4.6.

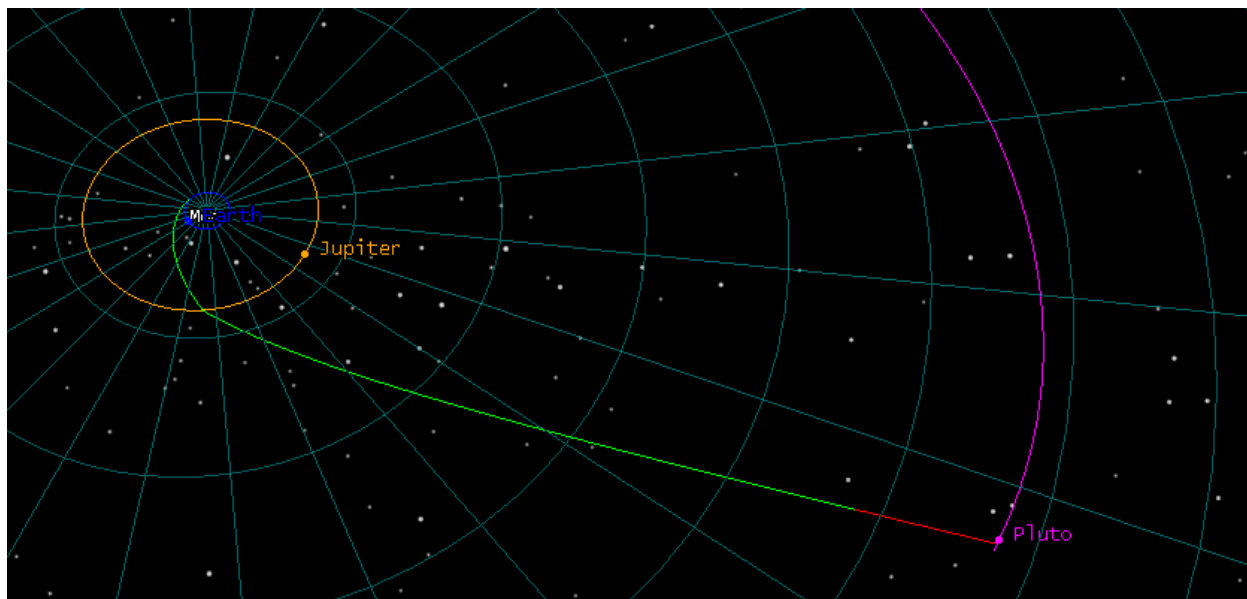


Figure 4.5: Interplanetary Trajectory - Ecliptic Normal



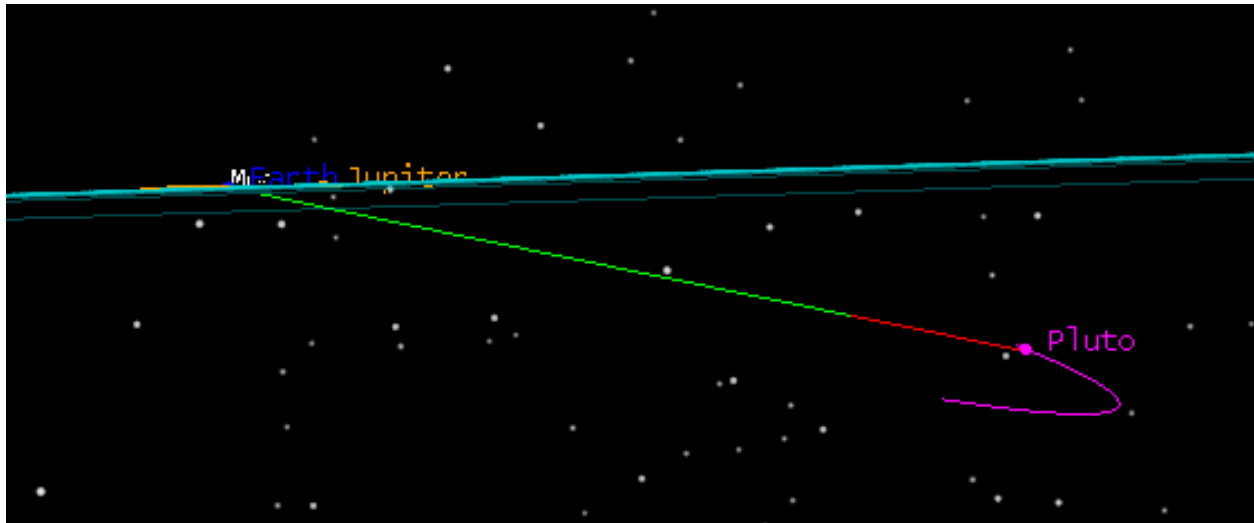


Figure 4.6: Interplanetary Trajectory - Ecliptic View

#### 4.4 Jupiter Gravity Assist

After the first cruise phase, the spacecraft encounters Jupiter and performs a JGA. This JGA is utilized for two primary reasons. First, the spacecraft gains some additional velocity via its encounter with Jupiter's gravitational field. This velocity increase serves to significantly cut the arrival time to Pluto. Second, the spacecraft changes its orbital inclination out of the solar ecliptic so that it can target Pluto. Without the JGA, this type of maneuver would consume an extraordinary amount of fuel. Instead, this maneuver requires no fuel expenditure on behalf of the spacecraft. By simply flying by the gas giant, the spacecraft gains enough velocity and inclination change to achieve the mission. This helps to reduce the requirements of the propulsion system.

Using STK, Jupiter can be targeted via a method commonly known as B-Plane targeting. For interplanetary missions, an imaginary B-Plane can be attached to any central body. This plane passes through the center of the body and is perpendicular to the incoming trajectory vector. By targeting certain points on this plane, a gravity assist can be performed, which accomplishes the velocity and inclination requirements of the trajectory. Visualizations of the geometric composition can be seen in Figures 4.7 and 4.8.

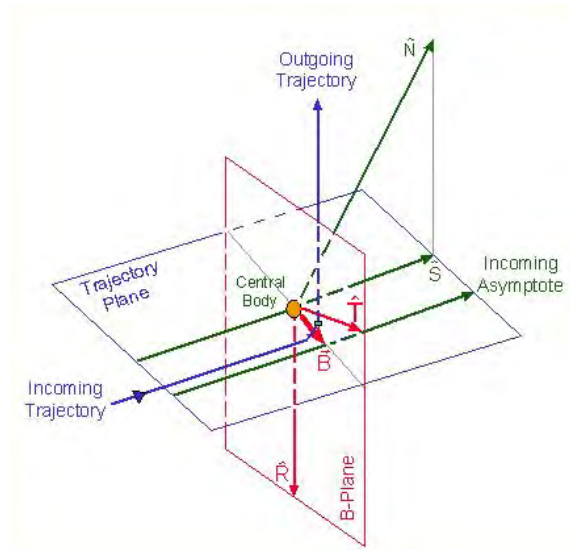


Figure 4.7: B-Plane Definition [15]

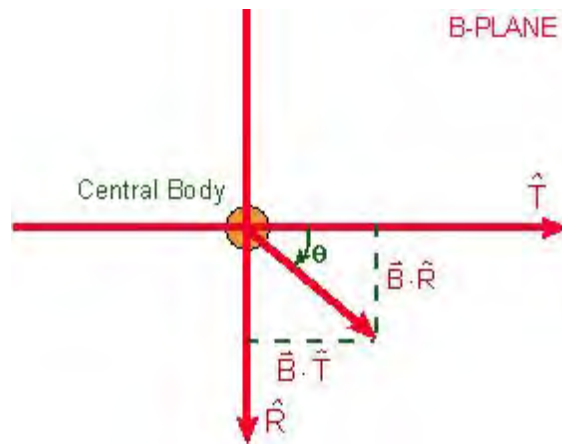


Figure 4.8: B-Plane Vector Components [15]

For B-Plane targeting, it is easy to think of the  $B \cdot T$  component as the one that increases or decreases the spacecraft velocity and the  $B \cdot R$  component as the one that changes the inclination of the orbit. In reality, these two components are coupled to one another as the  $R_{mag}$  value, which is calculated as the hypotenuse of these two components and determines how strong of a gravitational force the spacecraft experiences.

The parameters for the JGA can be seen in Table 4.6 and visualized in Figures 4.9 and 4.10.

Table 4.6: JGA Parameters

Flyby Date	30 June 2031
$R_{mag}$	16,379,700km
$B \cdot R$	-437,068km
$B \cdot T$	2,579,231km

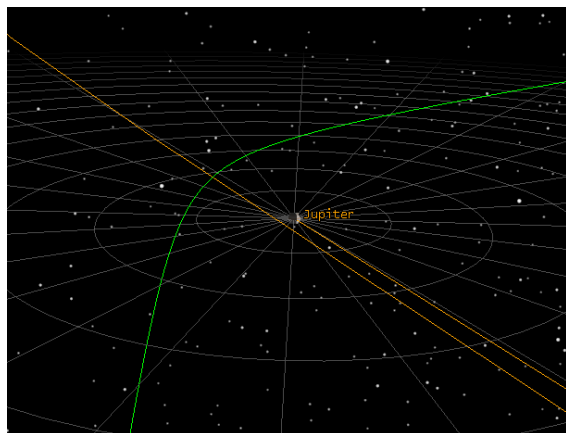


Figure 4.9: Jupiter Gravity Assist

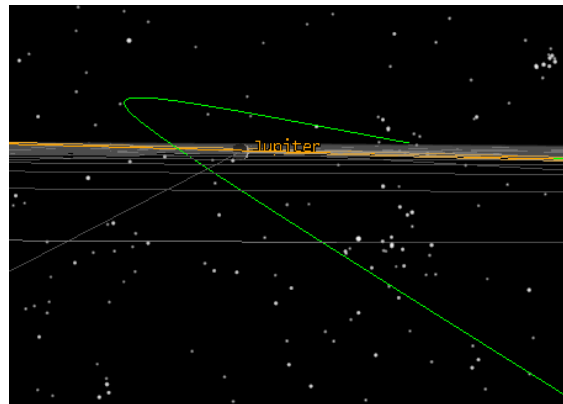


Figure 4.10: Jupiter Gravity Assist - Ecliptic View

The flyby radius of this maneuver is very large, and the flyby occurs over the course of a few days; however, due to Jupiter's large magnetic field, there are a few precautions that must be considered. Jupiter has a large magnetosphere which is significantly influenced by the solar wind, Jupiter's internal magnetic field, and Io, which exerts a large amount of sulfur dioxide. Jupiter's magnetosphere is composed of many complex structures: the bow shock, magnetopause, magnetosheath, and other components. The bow shock of the Jupiter extends to about 82 radius of Jupiter while the magnetopause has a distance between 50 to 100 radius of Jupiter. In the magnetopause, the region is filled by circulating plasma due to Io's volcanic sulfur dioxide eruption as well as Jupiter's rotation [16][17].

Jupiter's magnetic field is also large enough that it must be considered as a significant disturbance factor in the spacecraft altitude. The magnetic torque must be countered by the attitude control system in order to maintain the spacecraft's pointing direction. Further analysis of this phenomenon will be discussed in Section 6.8.2.

## 4.5 Pluto Orbit Insertion

For Pluto orbit insertion (POI), spacecraft speed must be significantly reduced. To do this, there are two primary approaches. In the first approach, the spacecraft reduces its arrival velocity significantly and follows a very standard orbit insertion procedure. While carrying significant risk, the second approach

reduces the need to lower the arrival velocity as much. Instead of completely slowing down the spacecraft with the propulsion system, the spacecraft can instead have a slightly higher arrival velocity and use a Charon gravity assist to slow down the last amount for orbit insertion. However, because of the low mass of Pluto and Charon, only about 1-2 km/s can be provided to the spacecraft via this maneuver.

Given the difficulty of accurately targeting Charon for the flyby and the long communication delays experienced far into the solar system, the risk for using a Charon gravity assist is deemed too high to use for POI. Any error in targeting during this maneuver would result in ejection from the system and an irreversible trajectory.

Utilizing an electric propulsion system, the spacecraft performs a long-duration capture maneuver to reach the necessary Pluto arrival velocity. After 3.6 years of near-constant thrusting, the spacecraft velocity is reduced to capture speeds of roughly 0.5 km/s. On February 6, 2047 the spacecraft enters Pluto orbit after expending 711 kg of fuel. This initial insertion is shown in Figure 4.11.

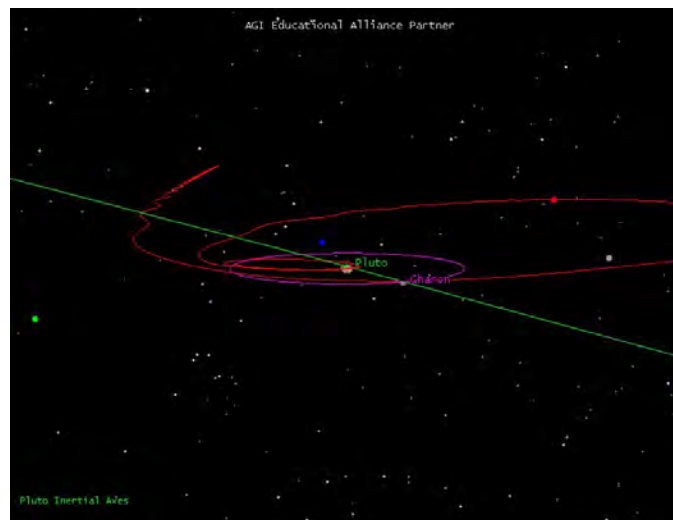


Figure 4.11: Pluto Orbit Insertion

After this initial insertion, the electric propulsion system will continue to lower the apoapsis of the orbit so that more consistent observations can be made of Pluto. This also minimizes the Charon gravity interactions for the initial phase of the mission as the primary scientific interest lies with further Pluto observations.

## 5 Primary Mission

### 5.1 Design Methodology

In its simplest form, the primary mission can be broken into three phases chronologically: Pluto observation, small satellite observations, and Pluto departure. While in reality scientific observations will be mixed throughout the various phases, this decomposition allows for objective prioritization and more precise mission planning. Given the event of a primary spacecraft failure, it is critical that the most important scientific data is gathered and relayed back to Earth first. Thus, Pluto observations are prioritized in the first mission phase before the focus is shifted to its other satellites. At the end of the mission, Pluto deorbit is required so that the spacecraft can head back towards the inner solar system. This maneuver is required due to the low data rate of the communications system. A detailed analysis of this design rationale can be found in Section 6.6.

In reality, mission design is extremely complex and continuously changes as scientific data is relayed back to Earth. This analysis is intended to provide a fundamental, baseline approach to the mission design which can be built off of. By providing only the fundamental concepts and leaving the detailed mission design to be determined as the spacecraft makes its groundbreaking scientific discoveries, further emphasis can be placed on mission reliability and success.

### 5.2 Phase 1: Pluto Observation

The first mission phase will begin during the POI maneuver and continue for the first few years of the orbital mission. A highly inclined orbit of 85 deg will allow for an extensive Pluto ground-track which enables thorough scientific observations. The initial orbit will maintain an apoapsis of 8,500 km and a periapsis of 3,000 km. By keeping the apoapsis below Charon's orbit, its gravitational perturbations are minimized and the spacecraft can focus on predictable observations with minimal orbital correction maneuvers. Using STK to observe the system dynamics, it was discovered that by keeping the orbit apoapsis at or below 16,000 km served to minimize the Charon gravitational perturbations while still allowing observations of Charon's tidally-locked face. In addition to the Pluto and Charon observations

during this phase, the descent probes will also be deployed. Two of the probes will be used to target geologically active regions of Pluto's Sputnik Planum. Given the success of these probes, the third descent probe will be deployed to investigate Charon's north pole. In the event that additional data is required of Pluto's surface, the third descent probe will serve as a backup.

Direct observations of Pluto will be initiated primarily near periapsis of the orbit with the rest of the orbit dedicated to data relay and spacecraft maintenance. Conversely, Charon observations will be initiated near apoapsis with spacecraft data transmissions occurring near the orbit periapse. Figure 5.1 shows the first month of the orbit after orbital insertion. At an apoapse of 8,500 km, Charon's gravitational perturbations are still noticeable. While these perturbations are not significantly detrimental to the mission, continual correctional maneuvers will have to be performed throughout the mission.

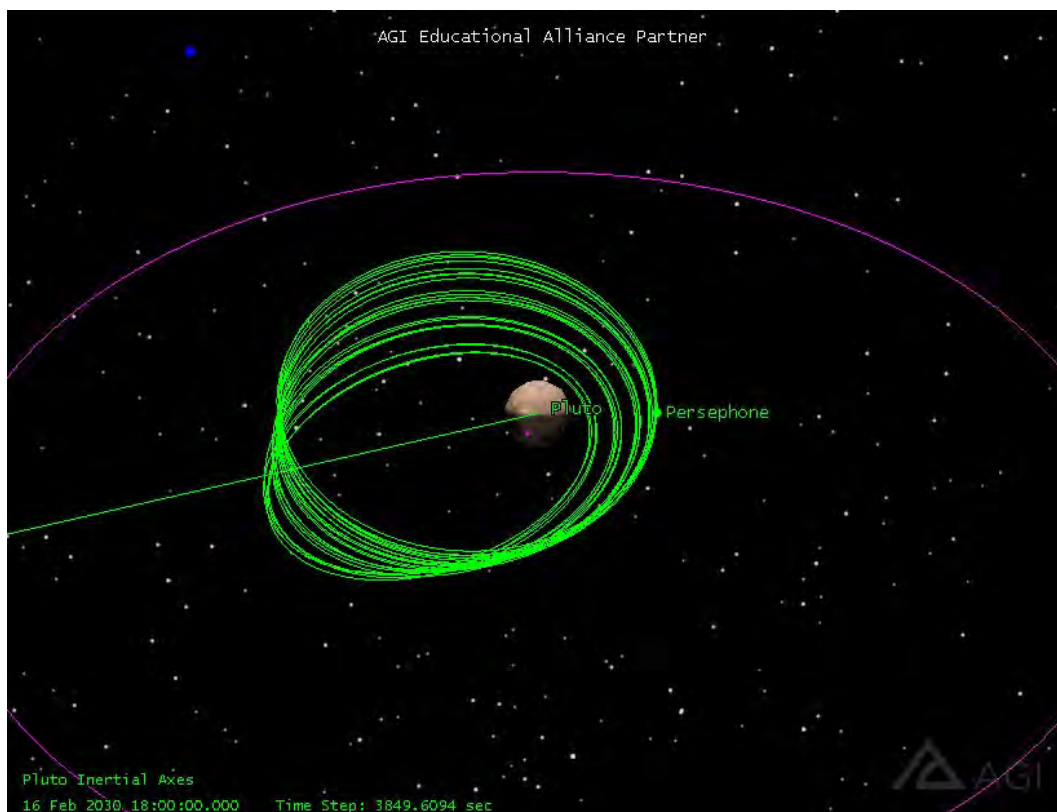


Figure 5.1: First Month of Orbit

During this phase, a plentiful amount of scientific observations can be conducted. The GCMS and SWAP instruments require close passes to Pluto's atmosphere to take measurements of its composition and its escape rate. These instruments will collect the most data during Phase 1. Additionally, Ralph will operate during this phase when power is available. The low orbital altitude of this phase provides the best opportunity to detect any thermal anomalies below the surface and take the closest images of Pluto. For the RSS instrument, experiments occur whenever data is transmitted back to Earth. Therefore, it is operating at any point where the radio signal is being relayed back to Earth. The important action of the RSS is to send signals at a variety of different points during the spacecraft orbit so the Doppler shift can be detected from these various points.

### **5.3 Phase 2: Observation of the Moons of Pluto**

Phase 2 will consist of a more in depth observation of Charon and focus on the other moons of Pluto. With Phase 1 limited to only observing Charon's tidally locked face, further observations and mapping of its surface are desired. Additionally, very little information is known about Pluto's smaller satellites. This phase will focus on enabling these scientific observations which will allow for significant discoveries to be made.

#### **5.3.1 Charon**

After Phase 1, the spacecraft will boost the apoapsis to 25,000 km which raises the orbit above Charon's orbital radius. This will allow for observations of the many unmapped regions of Charon, primarily the poles. This orbit gives a nearly harmonic response, and the spacecraft will be able to observe Charon nearly every orbit while utilizing Charon's gravitational pull to its advantage. The first few orbits of this phase can be seen in Figure 5.2.

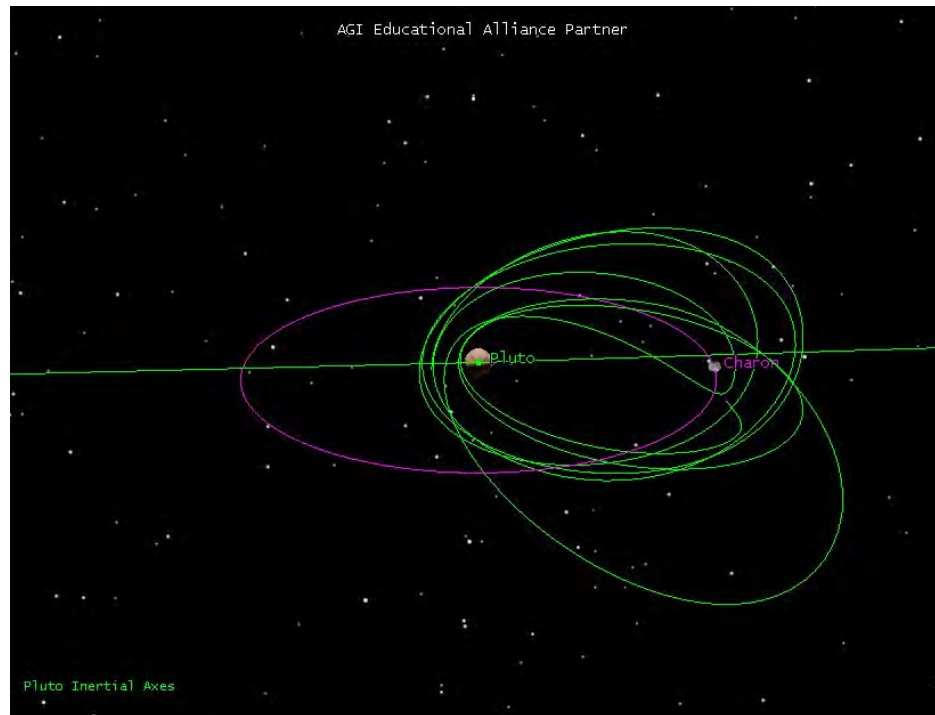


Figure 5.2: Charon Observation

Scientifically, using Ralph to map Charon's far side is the most important part of this phase. Once a high resolution map has been generated, the spare descent probe may be deployed if it has not already been used. The GCMS and SWAP instruments will be turned on when in contact with atmospheric particles that are being captured by Charon. These scientific observations will provide great insights into the role Charon plays in Pluto's atmospheric escape as well as the deposition of tholins near its northern pole.



### 5.3.2 Styx

Styx is the least well-known moon of Pluto. The preferable approach to observing Styx would be the same as Charon, but Persephone spiral outwards to an apoapsis of 36,000 km and approach the moon from that distance. Once it has been reached, the main scientific objective will include taking photographs and determining what scientific experiments are to be performed on the moon once more is known about it. A sample of this orbit is shown in Figure 5.3.

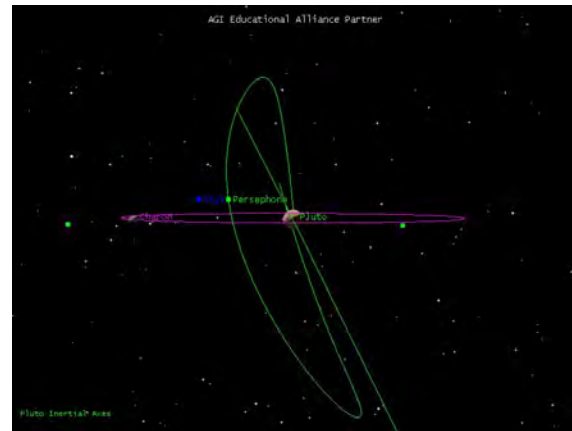


Figure 5.3: Styx Observation (Styx in Blue)

### 5.3.3 Nix

A similar approach will be used for Nix. This orbit apoapsis will be roughly 70,000 km and will allow Persephone to perform extremely close passes to study the moon. Since Nix is the most studied small moon of Pluto, it may be possible to determine areas of scientific interest beforehand and then perform them as Persephone approaches Nix. A sample of this orbit is shown in Figure 5.4.

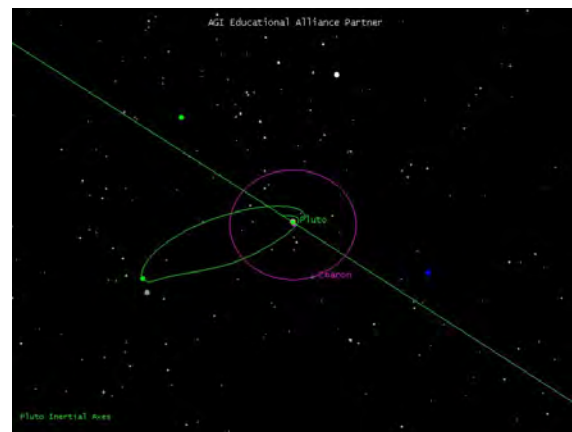


Figure 5.4: Nix Observation (Nix in Gray)

### 5.3.4 Kerberos

Kerberos is as unknown as Styx when it comes to the Pluto system. A similar approach method will be used as with the previous moons, but at an apoapsis of 200,000 km since it is much more distant than the others. Similar to Styx, it will be important to first map the surface of Kerberos and then determine what scientific studies will be done on the subsequent orbits. A sample of this orbit is shown in Figure 5.5.

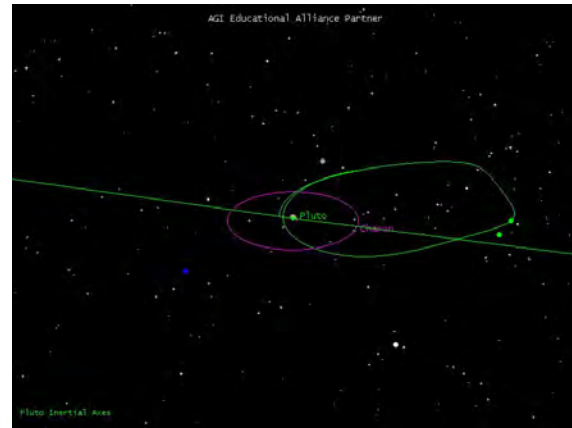


Figure 5.5: Kerberos Observation (Kerberos in Lime Green)

### 5.3.5 Hydra

Lastly, Hydra will be observed. This will require an apoapse raise to 300,000 Km. Hydra is also mapped in a quality equal to Nix; therefore, it may be possible to determine an area of interest before its approach to conduct scientific experiments. A sample of this orbit is shown in Figure 5.6.

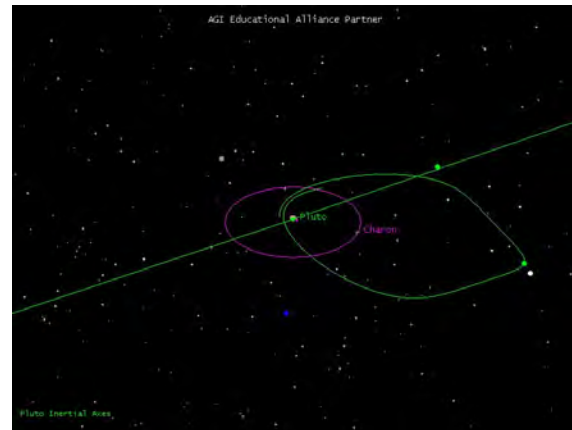


Figure 5.6: Hydra Observation (Hydra in yellow)

## 5.4 Phase 3: Pluto deorbit

Phase 3 will conclude the spacecraft primary mission. Once observation of the moons are done, the spacecraft will return to a solar orbit and lower its periapse to approach Earth. In order to obtain a sufficient data rate for the data transmission, the spacecraft must reach a distance close to that of Jupiter's orbit. Without this phase, it would take an immense amount of time and resources to relay all of the data back within the spacecraft lifetime.

Unlike with POI, the risk of using a Charon gravity assist is significantly less due to the extensive time on orbit and lower relative speeds. By using Charon to slingshot out of the Pluto system, the spacecraft will begin its journey back into the inner solar system. This maneuver is shown in Figure 5.7. Using the leftover propellant, the spacecraft will accelerate the spacecraft back towards the Sun to minimize the time it takes to complete this phase.

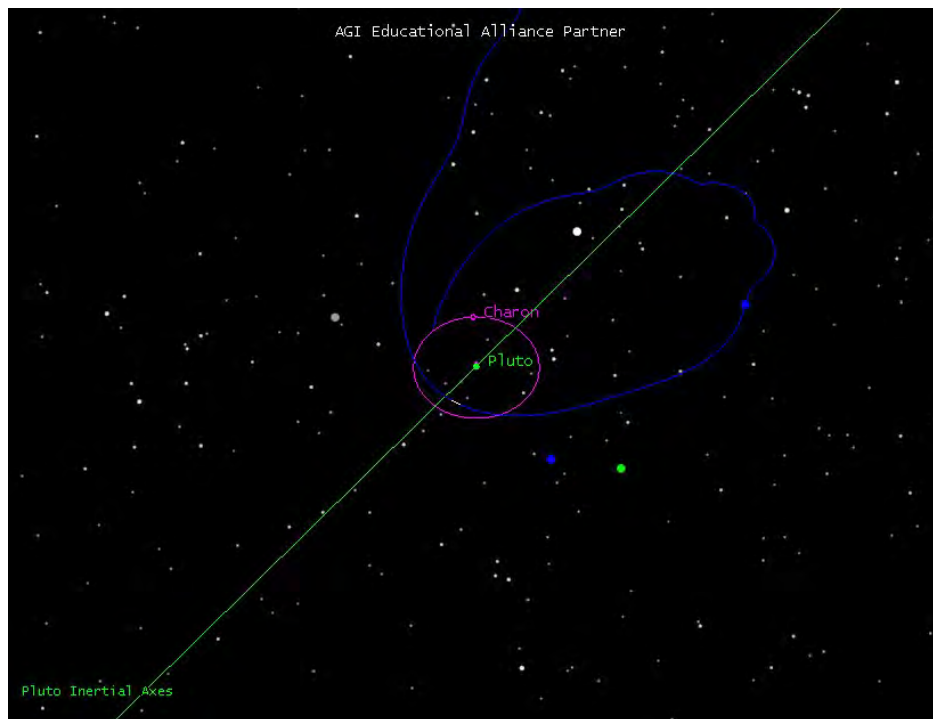


Figure 5.7: Pluto deorbit

## 5.5 Secondary Mission Potential

The spacecraft primary mission officially ends on January 7, 2050. Due to the necessity to deorbit Pluto in order to relay the scientific data back to Earth, the possibilities for a secondary mission are very limited. Primarily, any secondary mission would include a simple mission extension to allow further observations within the Pluto system.

## 5.6 Spacecraft Disposal

In the event of catastrophic failure, Pluto is rated as Class II via NASA's Office of Planetary Protection. Given this classification, a crash into either Pluto or any of its satellites would be permissible. However, if this were to occur, areas of little scientific interest would be targeted given that the spacecraft maintains enough control authority to enable this decision.

## 6 Spacecraft Design

### 6.1 Configuration & Overview

The Persephone spacecraft design focuses on maintaining symmetry along the longitudinal axis. This configuration allows for spin-stabilization of the spacecraft during its long interplanetary cruise period, which reduces the requirements placed on the attitude control system. An overview of the spacecraft configuration can be seen in Figures 6.1—6.4.

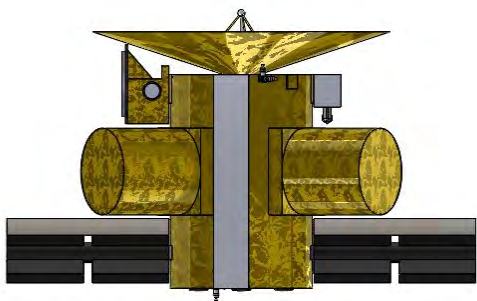


Figure 6.1: Spacecraft Configuration—Front

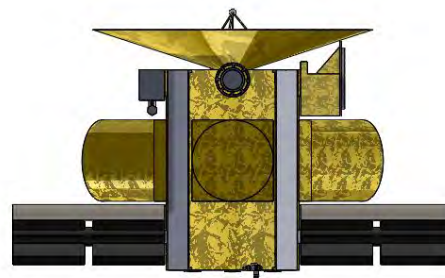


Figure 6.2: Spacecraft Configuration—Back

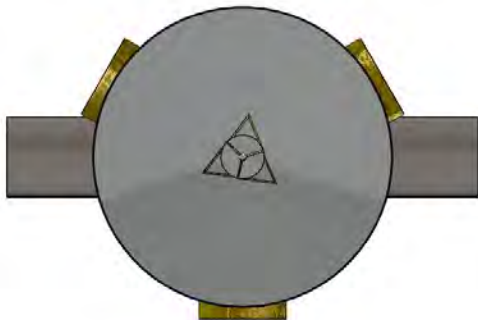


Figure 6.3: Spacecraft Configuration—Forward

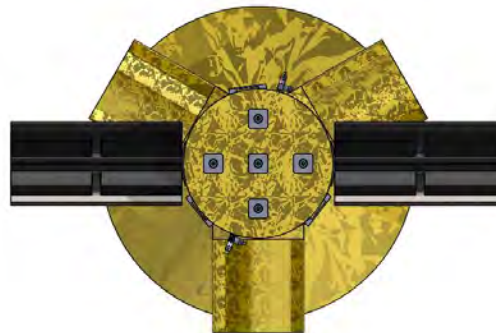


Figure 6.4: Spacecraft Configuration—Aft

The spacecraft's primary power comes from two General Purpose Heat Source (GPHS) Radioisotope Thermoelectric Generators (RTG), which are located near the aft end of the bus. Radiation shields are mounted above to reduce the affects of the radioactive decay on the rest of the spacecraft components, primarily the electronics and scientific instruments. Five low-power BHT-600 Hall effect thrusters serve as the primary propulsion system, and the incorporation of five allows for three-fault tolerance of the propulsion system as well as the ability to provide two-axis attitude control if desired.

The 1.5 m high-gain antenna (HGA) mounted on the bus forward end operates in the Ka band to relay data to Earth. A 0.3 m medium-gain antenna located inside the HGA has a lower data-rate and serves as a redundant system. Around the middle of the bus, three descent probes encapsulated by separate casings enable the atmosphere and geology of Pluto and Charon to be explored. Forward of these probes, the remaining scientific instruments are mounted. Running the length of the spacecraft bus, three radiators allow for heat rejection. A reaction control thruster triad is located at each end of the bus to maximize the moment arm and enable better attitude control. Figure 6.5 shows the interior of the spacecraft.

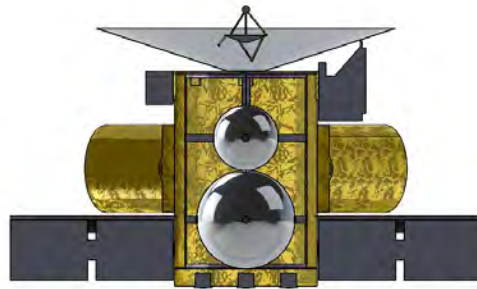


Figure 6.5: Persephone Spacecraft Cutaway

The primary propellant tank contains the iodine propellant needed for the mission and is located at the aft end of the bus. Mounted above this tank is the hydrazine propellant tank. All spacecraft electronics and additional systems are mounted on the forward plate.

The overall mass budget of the spacecraft can be seen in Table 6.1. Per the RFP, the spacecraft must maintain a dry mass less than that of New Horizons at 278 kg, neglecting the propulsion system.

Table 6.1: Spacecraft Mass Budget

<b>Component</b>	<b>Mass (kg)</b>
<b>Scientific Instruments</b>	
Ralph	10.50
SWAP	3.30
RSS	0.50
Descent Probe ( $\times 3$ )	17.00
CAPS	12.50
<b>Structure</b>	
Aluminum Honeycomb Shell	12.00
Titanium Frame	37.60
<b>Propulsion</b>	
Propellant	870
Propellant Tank	0.5
Butek BHT-600 Thruster ( $\times 5$ )	14.00
Power Processing Unit ( $\times 4$ )	12.00
GPFS RTG	57.00
<b>Power</b>	
Shunts	0.20
Wires	3.00
Batteries	3.00
DC-DC Converter	2.00
<b>Command &amp; Data Handling</b>	
Flight Computer	3.00
Solid State Recorder	1.50
Micro SD Card ( $\times 500$ )	0.50
<b>Communications</b>	
High Gain Antenna	20.00
Medium Gain Antenna	4.00
Low Gain Omni-Antenna ( $\times 2$ )	4.00
TWTA	4.00
<b>Thermal Control</b>	
GPFS RTG	57.00
Radiators ( $\times 3$ )	7.50
<b>Guidance, Navigation &amp; Control</b>	
Hydrazine Propellant	25.00
Reaction Control Thruster Triad ( $\times 2$ )	6.00
Reaction Wheel Assembly	28.60
<b>Attitude Determination</b>	
Star Tracker ( $\times 2$ )	6.00
Adcole Fine Sun Sensor	1.50
Inertial Measurement Unit	4.70

Table 6.2 summarizes the mass budget.

Table 6.2: Mass Budget Summary

Dry Mass ( <i>kg</i> )	275.90
Propulsion System Dry Mass ( <i>kg</i> )	83.50
Propellant Mass ( <i>kg</i> )	870
<b>Total Mass (<i>kg</i>)</b>	<b>1229.40</b>

The spacecraft dry mass remains below the maximum allowed value. Adding the propulsion system significantly increases the overall mass of the spacecraft. However, this mass is needed to allow for POI.

## 6.2 Structure

In the space environment, forces acting on the spacecraft structure are on the magnitude of millinewtons. The largest forces experienced by the spacecraft over its entire lifetime occur during Earth launch. Thus, the spacecraft structure must be designed to survive these large loads. The accelerations provided by the SLS to the payload are shown in Table 6.3.

Table 6.3: SLS Payload Accelerations

	<b>Liftoff</b>	<b>Transonic</b>	<b>Max Q</b>	<b>Max G Core</b>
<b>Axial (<i>g</i>)</b>	2.75	2.00	2.50	3.50
<b>Lateral (<i>g</i>)</b>	0.75	0.75	0.50	0.25

To reduce the spacecraft mass, an aluminum honeycomb composite primary structure is used to contain all spacecraft subsystems and aid the thermal control system by enabling the "thermal bottle" technique; however, the use of this lightweight structure does not provide sufficient compressive strength to survive launch loads. To provide a lightweight yet effective solution, a titanium frame, shown in 6.6, is mounted inside the aluminum honeycomb structure to take all of the compressive loading from launch. Due to its high specific strength and common use in aerospace applications, titanium 6Al-4V is used.





Figure 6.6: Titanium Frame

### 6.3 Propulsion

To achieve an orbital class Pluto mission, the propulsion system must be robust, reliable, and efficient. A variety of new, cutting edge propulsion systems have great potential for future deep space missions; however, only propulsion systems that have a technology readiness level (TRL) of 6 or higher are considered for this mission. Table 6.4 provides a brief summary of TRL definitions as defined by NASA.

Table 6.4: TRL Definitions

TRL	Definition
1	Basic principles observed and reported
2	Technology concept and/or application formulated
3	Analytical and experimental critical function and/or characteristic proof-of-concept
4	Component and/or breadboard validation in laboratory environment
5	Component and/or breadboard validation in a relevant environment
6	System/subsystem model or prototype demonstration in a relevant environment (ground or space)
7	System prototype demonstration in a space environment
8	Actual system completed and "flight qualified" through test and demonstration (ground or space)
9	Actual system "flight proven" through successful mission operations

The spacecraft propulsion system provides a few key critical functions to the mission. First, coupled with the launch vehicle, it provides the spacecraft with enough energy throughout the mission to reach the Pluto system in a reasonable amount of time. Second, it enables the spacecraft to capture into orbit around Pluto upon arrival. Lastly, the propulsion system must support mission operations while on Pluto orbit to obtain scientific data and relay it back to Earth. In addition to these three functions, it is critical that the system be extremely reliable for the entirety of the 25 year baseline mission. Failure of the propulsion system would result in either complete loss of the spacecraft or substantial losses to the scientific data collected throughout the mission.

### 6.3.1 Engine Type

From the dawn of the space age, spacecraft were limited to the use of chemical in-space propulsion systems. Chemical propulsion systems provide excellent performance and reliability for spacecraft and are by far the most well-tested propulsion system available; however, while chemical propulsion systems provide high performance and reliable operations in space, their applicability is well defined and not very flexible. In more recent years, a variety of new propulsion systems have been tested and show promise for present and future applications in space. Figure 6.7 shows the performance of different propulsion systems.

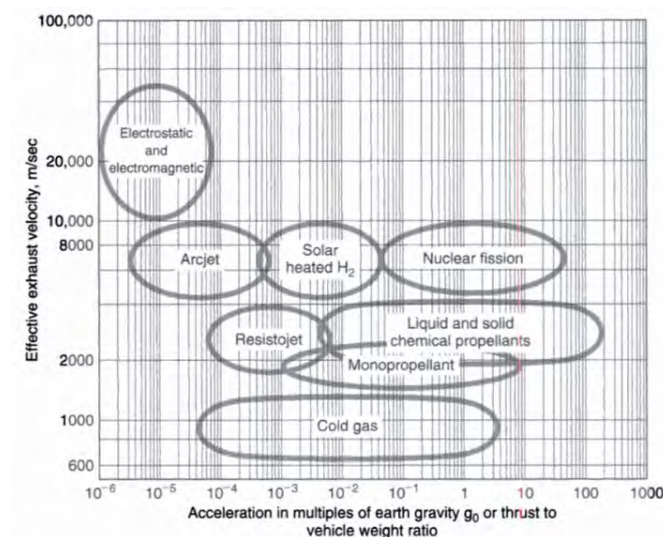


Figure 6.7: Propulsion Systems Performance [18]

Electric propulsion systems are the most popular and well tested of these new technologies. These systems provide increased efficiency to deep space applications by separating the power source from the propellant; however, this comes at the expense of lower thrust generation, leading to long acceleration times. Current state-of-the-art (SOA) electric propulsion systems have ISPs around 3,000-8,000 seconds and thrust on the order of 20-200 mN. Electric propulsion systems can be separated into two primary categories: solar and nuclear.

Solar electric propulsion (SEP) is the better tested and flight-proven of the two technologies. By using solar arrays, spacecraft in the inner solar system can obtain vast amounts of power to use for these systems. The Juno spacecraft is a prime example of deep space solar power use, setting the record for solar array use deep into the solar system [19]. While Juno does not use SEP, the solar array technology demonstration expands the operational window for SEP use deeper into the solar system; however, the fundamental inverse square relation of solar flux to distance severely limits its use, requiring exponentially increasing array size. With the Persephone propulsion system requiring significant use near Pluto to attain capture speeds, this technology is severely limited for the mission.

Unlike SEP systems, nuclear electric propulsion (NEP) does not rely on the Sun to generate power, and instead it relies on internally generated power. This power can come in the form of either a nuclear reactor or an RTG. The use of a nuclear reactor allows immense amounts of power to be generated, but at the expense of a large system mass. The last and only nuclear reactor the US has ever flown in space was for the System for Nuclear Auxiliary Power (SNAP) program in 1965. This reactor produced 650 W of electrical power and had a reactor mass 435 kg. This mass does not include the supporting systems needed for the system to operate, including the radiators to dispose of the excess heat and the radiation shielding needed to protect the spacecraft. Using an RTG as the power source, the propulsion system would be able to operate at a comparable power with a system mass of only 114 kg; however, this power would decay over time much more rapidly than a nuclear reactor would. Additionally, this power cannot be turned off and will be generated throughout the mission even if it is not needed.

Nuclear Thermal Rockets (NTR) provide a unique compromise between performance and efficiency for the propulsion system, with thrust on par with chemical engines but an ISP much more like an electric

propulsion system. In the 1950s, NASA began extensive investigation into NTR use for deep space missions. This research eventually led to the development and test of the Nuclear Engine for Rocket Vehicle Application (NERVA), and this engine successfully proved the viability of NTR technology for future space missions, but for long-duration deep-space missions there are concerns with propellant storage. Using hydrogen as fuel, the large propellant volume and cryogenic storage temperatures are a major concern. With a high arrival velocity at Pluto, a large amount of fuel is needed to allow for orbit insertion.

Trade studies for these propulsion systems provide insight into the benefits and limitations of each. The ability to provide enough  $\Delta V$  for POI allows for relative comparison between the propulsion types. Providing the needed performance while maintaining low system mass and minimizing the interplanetary mission duration are the primary criteria for system selection. Comparison between chemical and NTR propulsion will be conducted first. Using a basic MMH-NTO chemical engine and the NERVA NTR, the engine parameters used are shown in Table 6.5.

Table 6.5: Chemical & NTR Engine Comparison

	<b>Chemical</b>	<b>NTR</b>
Propellant	MMH/NTO	$H_2$
ISP ( $s$ )	315	925
Thrust ( $N$ )	490	$333 \times 10^3$
Engine Mass ( $kg$ )	20	8,500

Comparing these engines over a variety of Pluto arrival velocities with a spacecraft dry mass of 300 kg, the results are shown in Figure 6.8.

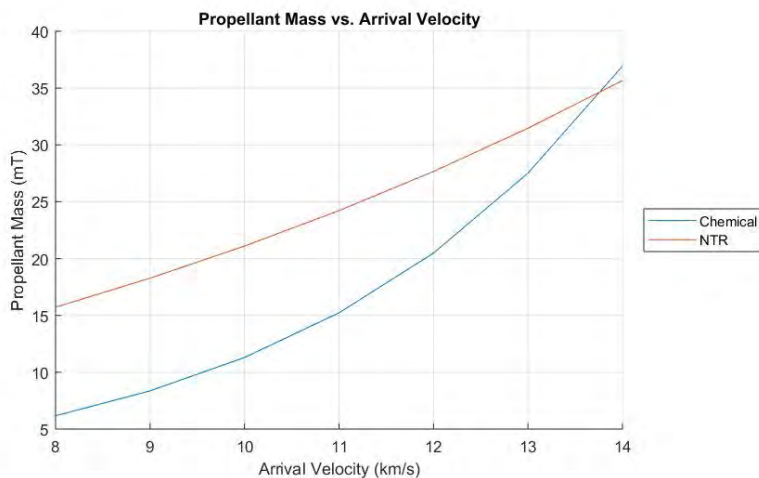


Figure 6.8: Required Propellant Mass

While an NTR engine provides better efficiency, the mass that the system adds to the spacecraft significantly inhibits its performance unless high arrival velocities are reached. With either system, it is obvious that both require a high propellant fraction to enable POI. While this is certainly doable, it is not necessarily ideal as it requires increased system mass and complexity.

Capture performance for electric propulsion systems was also analyzed. Utilizing the engine characteristics listed in Table 6.6, the performance can be seen in Figures 6.9 and 6.10.

Table 6.6: Electric Propulsion Engine Specifications

ISP ( $s$ )	1,725
Nominal Thrust ( $mN$ )	45
Beginning Maneuver Power ( $W$ )	500
Dry Mass ( $kg$ )	300
Propellant Mass ( $kg$ )	900

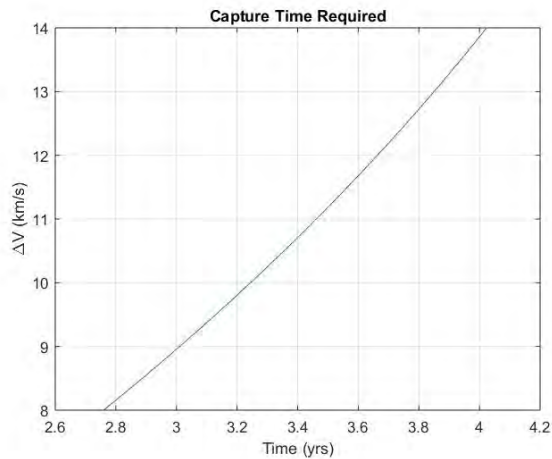


Figure 6.9: Required Maneuver Time

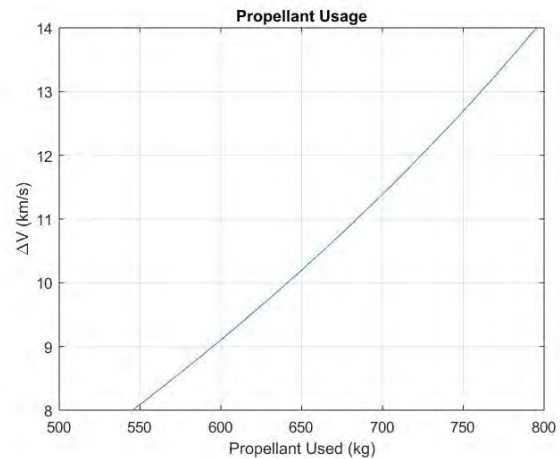


Figure 6.10: Propellant Usage

Using electric propulsion significantly decreases the propellant mass needed to perform the POI; however, this comes at the expense of a long capture maneuver. The concern with using electric propulsion originates from the steady-state burn time allowed for low-power propulsion systems. This can be partially mitigated through the use of multiple engines, but it is still a primary failure mode that is potentially catastrophic to the mission.

The electric propulsion performance significantly depends on the power source utilized. For a SEP system, the power will decay primarily as a function of distance from the Sun. For a NEP system, the power will decay primarily as a function of time given an RTG power source. These both have significant implications for the propulsion performance. Figures 6.11 and 6.12 compare the two power systems using a 500W power availability to the propulsion system at the start of the POI maneuver.

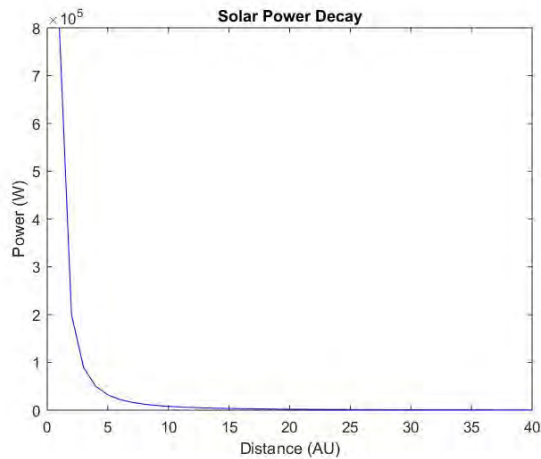


Figure 6.11: Solar Power Decay

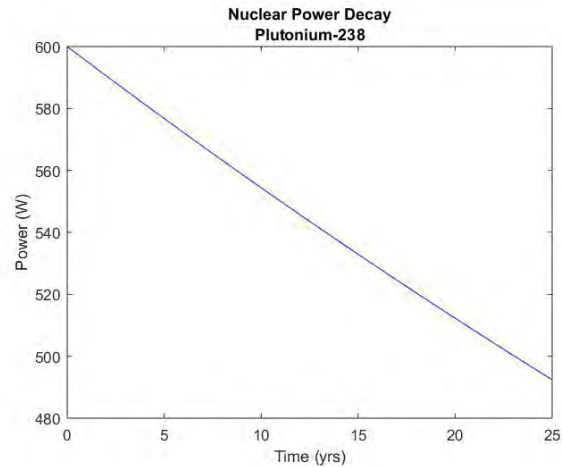


Figure 6.12: Plutonium Power Decay

Utilizing solar power requires an extremely large array size to capture 500 W of solar power near Pluto's orbit. At Earth orbit, the array would have to generate 800 kW of power. For high-power solar panels, a conservative specific power number of 60 kg/W gives an array mass of about 13,000 kg. This extremely large mass feeds back into the propellant mass needed and the POI duration, decreasing the effectiveness of the solution. By utilizing two GPHS RTGs, enough power can be provided to the propulsion system and adds only 114 kg to the spacecraft. Through the use of RTGs, an electric propulsion system can be a very practical solution.

Hybrid propulsion systems provide a unique solution to reduce spacecraft mass as well as mission duration. In this case, a chemical-NEP hybrid propulsion system is analyzed to determine its effectiveness. For this solution, the chemical propulsion system should provide the largest  $\Delta V$  possible without adding significant mass to the spacecraft. In this case study the chemical engine from Table 6.5 and the NEP engine from Table 6.6 are used. The combination of these two propulsion systems requires an iterative process to be used as the results from one system's performance feeds into the next. For this system, the NEP will slow down the spacecraft to a certain critical speed and then the chemical propulsion system will lower the remaining velocity to allow for POI. For lower  $\Delta V$  maneuvers, the chemical propellant mass needed is shown in Figure 6.13.

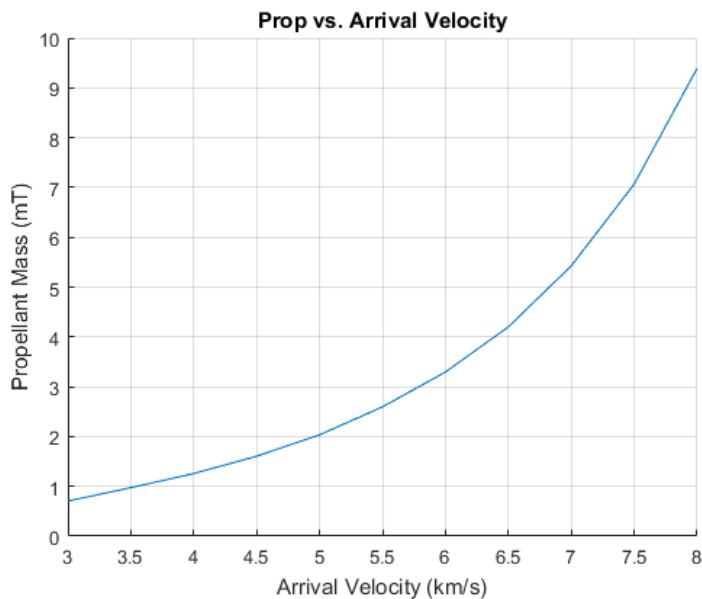


Figure 6.13: Hybrid Chemical Propellant vs. Arrival Velocity

Taking the  $\Delta V$  provided by the chemical propulsion system to be 4 km/s, the NEP system must provide a 7.7 km/s cumulative  $\Delta V$  to reduce the spacecraft velocity within before this maneuver is performed. The resulting NEP performance can be seen in Figures 6.14 and 6.15.

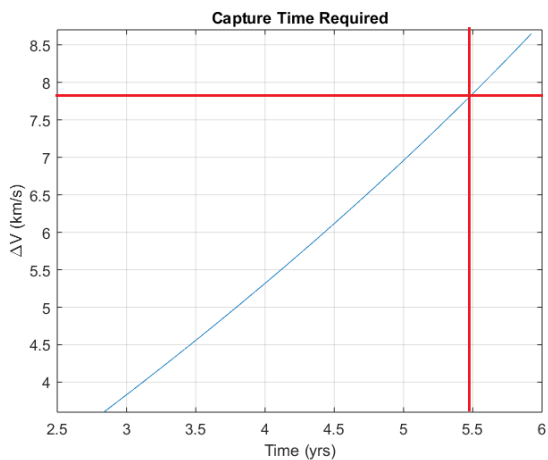


Figure 6.14: Hybrid NEP Capture Maneuver

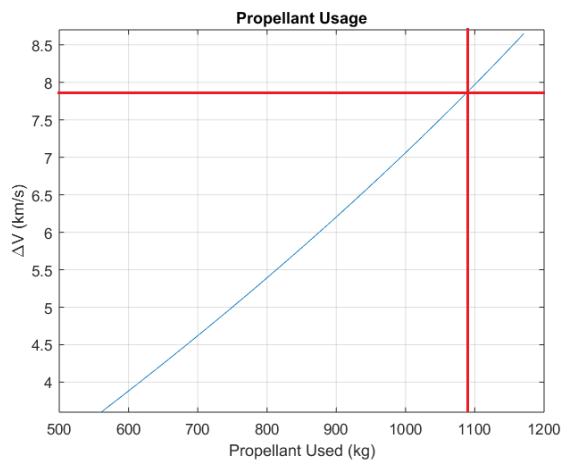


Figure 6.15: Hybrid NEP Propellant Usage



For a hybrid propulsion system, the required NEP maneuver duration increases to 5.5 years compared to the 3.6 years for the standalone NEP system because of the increased overall spacecraft mass. This duration increase only serves to increase the concerns of the steady-state firing time required on the system which remains a concern as a primary failure mode. Additionally, the implementation of a hybrid propulsion system does not significantly reduce the interplanetary trajectory duration but serves to add significant complexity to the spacecraft. Overall, the utilization of a hybrid propulsion system is not feasible for this mission.

After considering all potential solutions, a NEP propulsion system provides the most feasible and effective solution to the problem. Care will have to be taken to ensure that redundant systems alleviate the system failure concern due to the large maneuver durations.

### **6.3.2 Engine Selection**

With the decision to utilize an NEP system, the engine selection must be performed. A particularly limiting factor in engine selection is the low operating power available to the system. This constraint narrows the potential engine options.

Engine operational history, thrust level, and operating power range drove the engine selection process. With a long deceleration maneuver, a proven extended operational capability is critical to mission success. After running multiple simulations in STK, it was clear that high thrust must be prioritize to minimize the strain on the system; however, there is an inverse relationship between the thrust provided and the ISP of the engine. This relationship must be carefully evaluated as too low of an ISP would increase the spacecraft mass via added propellant and reduce the effectiveness of the increased thrust. Lastly, the power throttle range is a critical to ensure engine operation throughout the entire mission life. Using RTGs as the primary power source, the available power will be relatively low and will change over the mission duration. Thus, the selected engine must be able to operate over a power range that the RTG can reasonably provide.

A number of low power electric engines are considered for mission use. The engine specifications for these engines are shown in Table 6.7.

Table 6.7: Electric Engine Specifications

	<b>BHT-600</b>	<b>BIT-7</b>	<b>IHET300</b>
ISP ( <i>s</i> )	1,500	3,500	1,300
Nominal Thrust ( <i>mN</i> )	39	11	15
Nominal Power ( <i>W</i> )	600	360	300
Throttle Range ( <i>W</i> )	200 - 800	125 - 400	250 - 600
Mass ( <i>kg</i> )	2.8	1.6	1.6

Conducting an AHP analysis, these characteristics are used to determine the most effective engine for the mission. Table 6.8 shows the criteria weighting utilized and Table 6.9 shows the results from the AHP analysis.

Table 6.8: Criteria Weighting

<b>Metric</b>	<b>Weight</b>
ISP	0.1155
Nominal Thrust	0.4901
Nominal Power	0.2310
Throttle Range	0.1634

Table 6.9: Engine Selection

	<b>Weight</b>
BHT-600	0.4511
BIT-7	0.2663
IHET300	0.2826

From this study, the Butek BHT-600 engine is selected for use on the Persephone spacecraft. The lifetime of the engine must be examined to ensure its capability to perform the mission. From laboratory tests, a conservative lifetime of 10,000 hours has been established [20]. Given the 3.6 year capture maneuver, the minimum operating time required which does not include on-orbit operations is approximately 31,500 hours. Thus, to ensure mission success, a minimum of 4 engines are required without any redundancy.

A configuration of five engines addresses the reliability concerns that arise with the engine operational lifetime. These thrusters are placed in a "Plasma Plus" configuration, shown in Figure 6.17, that allows for three fault tolerance of the propulsion system. This tolerance allows for the reduction of system failure to 0.49% over the primary mission life. An added benefit of this configuration is the ability to use these engines for 2-axis attitude control given any failures in the attitude control system.

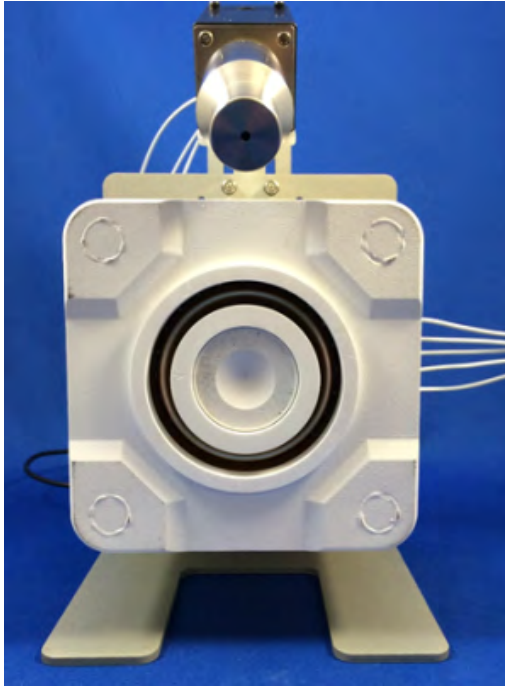


Figure 6.16: Butek BHT-600 Engine

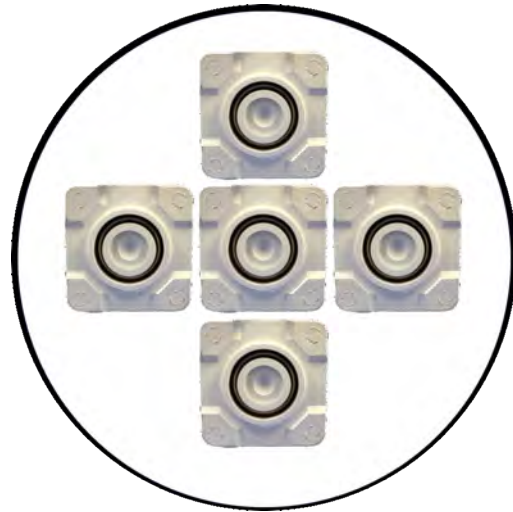


Figure 6.17: Thruster Configuration

### 6.3.3 Propellant Selection

The Butek BHT-600 engine is qualified for xenon, iodine, and krypton propellant use. Each of these propellants carry inherent benefits and risks. Without considering factors such as cost, performance, or workability, an optimization was performed for each propellant to size the tank. For this optimization, the cost function weightings are listed in Table 6.10, and the results of the optimization are shown in Table 6.11.

Table 6.10: Tank Optimization Weightings

	<b>Weight</b>
Tank Radius	0.3
Tank Mass	0.4
Storage Pressure	0.2
Propellant Fraction	0.1

Table 6.11: Propellant Tank Optimization

	<b>Xenon</b>	<b>Krypton</b>	<b>Iodine</b>
Storage Temperature ( $^{\circ}C$ )	21	21	21
Storage Pressure ( $psi$ )	172.5	172.5	7.3
Tank Radius ( $m$ )	1.442	1.666	0.345
Tank Thickness ( $mm$ )	1.868	2.158	0.019
Tank Mass ( $kg$ )	137.4	211.7	0.080
Propellant Fraction	0.861	0.801	0.999
Total System Mass ( $kg$ )	987.4	1061.7	850.1

Based on the optimization, using iodine propellant is the best choice from a mass and volume perspective due to its ability to be stored as a solid. Requiring an almost negligible storage pressure, the propellant can be stored in any volume and sublimated immediately before use. Iodine provides nearly identical performance to xenon propellant, making it a promising propellant for the mission.

While iodine would by far be the best selection given its mass and volume requirements, it is not without its faults. Iodine propellant has not been extensively tested in electric propulsion systems, leading to reliability concerns; however, initial tests of the BHT-600 engine using iodine propellant indicate no changes in thrust output [21]. Given the 12 years for technology development between the present and launch, longer-duration tests can be conducted to prove the propellant capability for long duration missions. With this time line, the benefits of using iodine propellant far outweigh the potential concerns.

## 6.4 Power

The demands placed on the power system are unique and never before has there been deep space probe utilizing electric propulsion. These unique demands have resulted in rather unique constraints on the system.

### 6.4.1 Generation

Current technology and the inverse-square law dictate that an RTG is used as the main power source for the mission. Two different and possible RTGs were compared. The MMRTG, which is NASA's

current standard and the GPHS-RTG, was recently retired in favor of the MMRTG. A minimum of 600 W at mission start are needed in order to meet the mission timeline and still have enough power at EOL to deorbit and bring Persephone closer to Earth. Table 6.12 compares the RTGs at the 600 W level.

Table 6.12: RTG Comparison

	Power	Weight	W/kg	Quantity	Total PU-238	Total Mass
<b>GPHS</b>	295 watts	57 kg	5.2	2	15.6 kg	114 kg
<b>MMRTG</b>	125 watts	45 kg	2.8	5	17.3 kg	225 kg

As is clearly visible in Table 6.12, using MMRTG presents a scenario where more PU-238 is required and have doubled the RTG mass compared to using the GPHS-RTG. While the difference in PU-238 might seem small, the difference is more PU-238 than will be produced in an entire year even when the Department of Energy achieves max PU-238 production rate in 2026. The higher mass of the MMRTG would also have severe implications on the mission timeline as it would increase the total mass of Persephone by approximately 10%. These two points led to the GPHS-RTG being chosen over the MMRTG even though the GPHS-RTG is retired. The fact that the chosen RTG is retired is not a major factor in the decision making process as the GPHS-RTG has been brought out of retirement previously and can be easily restarted again. The GPHS-RTG is shown in Figure 6.18.

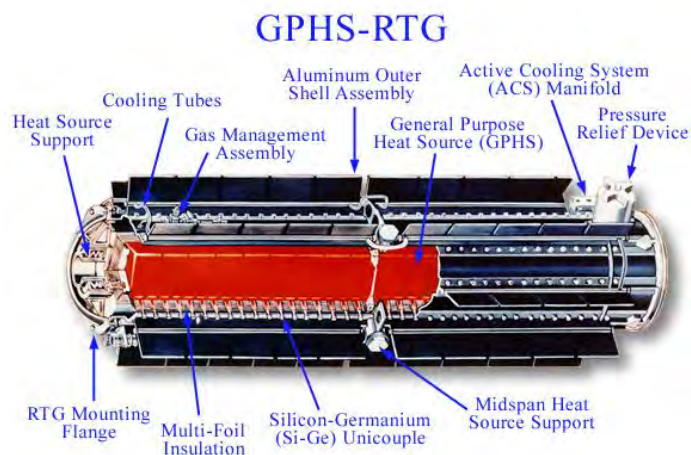


Figure 6.18: GPHS-RTG Cutaway

Another major system design consideration was the number of RTGs that the mission would use. About 600 watts of electrical power at mission start are needed, mostly due to demands placed by the propulsion system at EOL. System architectures with just 2, 3, or 4 RTGs were considered. Primarily due to the amount of Plutonium that would be needed in order to create each RTG, it was realized that the most viable option was to minimize the number of RTGs. This resulted in selecting the option to have just two; allowing the timeline to be met while minimizing the plutonium consumption. This trade comes at the cost of time of arrival at Pluto.

The power from the RTG will be regulated via a series of shunts that will turn the unneeded electrical power into heat which can be radiated away into space. This give the ability to easily switch between different power usage modes while still managing power in a highly reliable manner.

#### **6.4.2 Batteries**

Excess power from the RTG in various modes of operation will be used to charge a battery bank that can provide its stored energy to other subsystems to supplement the RTG power in modes where it is needed. For example, this will allow for more science payload usage simultaneously or to send data back at higher transmission rates. The battery chosen is the LI-PO BMU under development by NASA Johnson Space Center. This battery was chosen due to its extreme focus on safety. Any internal shorts are immediately resolved, and short of heating it up to well beyond 100 degrees Celsius, the battery is nearly indestructible.

### **6.5 Command and Data Handling**

The command and Data Handling system is responsible for processing all data, sending/receiving commands, executing commands, and storing all data. This system consists of a main computer, a short-term data storage system, and a long-term data storage system.

### 6.5.1 Main Computer

The main computer that chosen for Persephone is DDC's SCS750. This computer designed to be used in space and already has flight heritage. It is configured into a voting scheme with three processors using a simple majority vote to correct for errors. The SCS750 processor's details are in Table 6.13.

Table 6.13: DDC SCS750 Specs

Power Usage	MIPS	Mass	Rad Hardened?
7 - 30 Watts	200 - 1,800	1.5 kg	Yes



Figure 6.19: The DDC SCS750 computer

### 6.5.2 Short & Medium-Term Storage

Data will be stored in a solid state recorder capable of holding up to 1.5 terabytes of information. This will be used to store short and medium-term data. However, this will not be used to store all the data generated by the craft, and once used, data on this memory module will be deleted to create space for more data. To get 1.5 terabytes of data storage capability, three of the Southwest Research Institute's SSDs must be used. Together these SSDs weigh 1.5 kg, and are capable of data storage rates of 25 Gbps. [22]

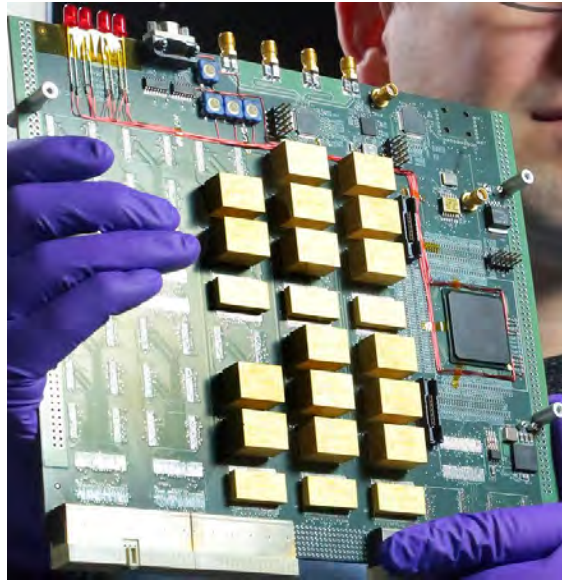


Figure 6.20: The Solid State Recorder

### 6.5.3 Long-Term Storage

Long-term data storage is paramount to the scientific success of this mission. There is a significant need to be able to store massive amounts. Specifically, the design target is 100 terabytes of data while maintaining low mass and remaining radiation tolerant. To solve this problem a fault-resistant architecture of microSD cards has been chosen. This option is not only capable of storing massive amounts of data in a tiny area, but it also consumes very little power, and can be scaled to any arbitrary radiation tolerance without having to develop any custom radiation-tolerant hardware by using N-Modular Redundancy.[23]

Using Integral's 512GB microSDXC V10, UHS-I U1 card as the benchmark, the system is designed. However, it is assumed a superior microSD card will be available within the next 4 - 5 years that can be used with higher data density. Table 6.14 shows the microSD card specifications used.[24]



Table 6.14: MicroSD Specifications

	Number Needed	Total Mass	Total Volume	Total Power
<b>Integral 512GB Model</b>	1000	1.0 kg	$675 \text{ cm}^3$	$0.3 \text{ Watts}$
<b>Assumed 1024GB Model</b>	500	0.5 kg	$337.5 \text{ cm}^3$	$0.3 \text{ Watts}$



Figure 6.21: Integral 512GB MicroSD Card

The architecture chosen is a 5-module redundant architecture as shown in 6.22. This architecture will guarantee that data integrity is always maintained even during intense ionization. Additionally microSD cards do not store their data magnetically, so the strong magnetic fields of the Jupiter system do not pose a threat to data integrity. There is an approximate read/write cycle max of 100,000 for each memory module on the microSD cards, however that limit should not be encountered due to memory management code that spreads the read/write cycles around, and the surplus of data storage available. Ensuring data integrity over the extended mission lifespan was the primary goal during design considering that the data storage device must survive 30+ years in order to recover all data.

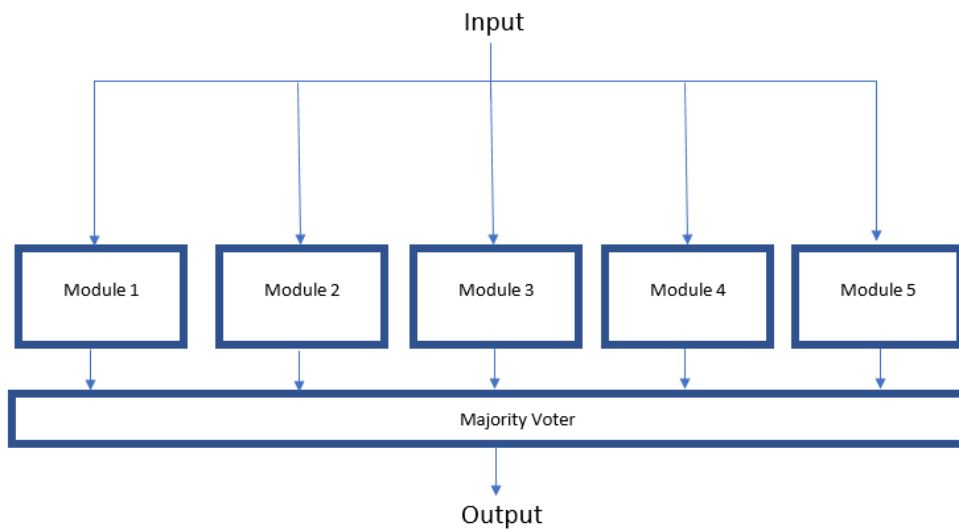


Figure 6.22: The 5-Module Redundant Data Storage Architecture

## 6.6 Communications

Communications at Pluto distances are incredibly limited. State-of-the-art science payloads collect an ever-increasing amount of data; however, the data return rates have been unable to keep pace with the amount of data generated. This leads to a problem for which there is currently no good solution. There is no way to send all of the data gathered in orbit around Pluto back in any sort of reasonable time frame. To illustrate this point, New Horizons operated its science package during its flyby of Pluto for less than a single day, yet it took 16 months to transmit all of that data back to Earth. These types of data rates are just unsustainable for an orbital probe. The reasoning for the deorbit maneuver outlined in Section 5.4 is explored in Section 6.6.4.

Persephone plans on using a communications system composed of:

- 1 high gain cassegrain antenna
- 1 medium gain parabolic antenna
- 2 low gain omni-directional antennas

### 6.6.1 High Gain Antenna

The high gain antenna used will be cassegrain type with a diameter of 2.5 meters operating in both X-Band and Ka-Band. By using both Ka and X band, Persephone will take advantage of the higher data rates offered by the Ka, while still allowing the use of heritage X-band communication devices that offer greater resistance to signal interference and help combat availability issues with the DSN. The antenna will have an average gain of 45 dBi throughout its nominal mission life and a half power beam width of 0.5 degrees. This give the ability to increase the data rates compared to what New Horizons was capable of (1900 bits/s) to nearly 10,000 bit/s. However, this data rate is still not nearly enough to send back all the data that will be gathered. However, it will allow for lower resolution data from each scientific instrument to be transmitted and at least accomplish the minimum scientific requirements.

The antenna will be made of ultra-light carbon composites, layered with a metallic reflector to keep the mass as low as possible. The high gain antenna will use two traveling wave tube amplifiers (TWTA) to

amplify the signal before it is fed into the horn. The TWTA's will utilize a left hand and right hand polarization scheme that increases the data rate to nearly double its baseline data rate.

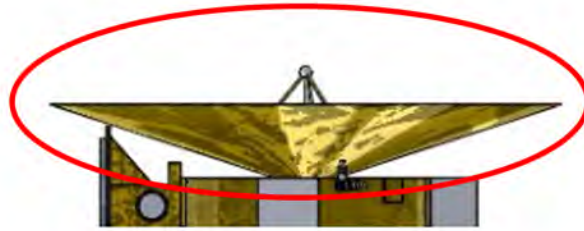


Figure 6.23: High Gain Antenna

### 6.6.2 Medium Gain Antenna

Persephone's medium-gain antenna will allow for better near-Earth communications and will allow it to communicate with the descent probes as they descend towards Pluto/Charon. The medium gain antenna will sit in the sub-reflector of the high gain antenna, reducing mass and operational complexity. As a result of its location, the medium gain antenna will be 34 cm in diameter.

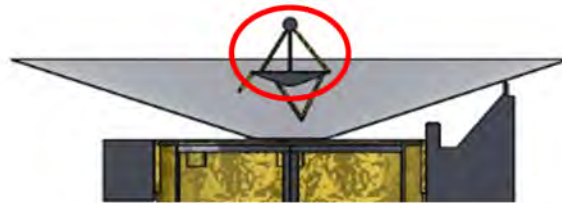


Figure 6.24: Medium Gain Antenna

### 6.6.3 Low Gain Antennas

Persephone will have two low-gain omni-directional antennas. These antennas will be used when near Earth and, more importantly, will allow the probe to receive messages from Earth when in deep space

regardless of the orientation of the probe. To accomplish this, the antennas will be placed on opposite sides of the probe, providing a complete 360-degree coverage around the probe. The low gain antennas will be 30 cm in length and will stick out from the side of the probe.

#### 6.6.4 Deorbit Reasoning and Calculations

Data rates at Pluto are so abysmally slow, that at the targeted data rate of 10,000 bits/sec, Persephone would need to be actively transmitting for  $\sim 25$  years just to return 1 terabyte of data. It's estimated that Persephone will generate  $\sim 5$  terabytes of data per year, so it does not take much to realize there is no way to send all the data back from Pluto using conventional communication systems, even accounting for data compression. This presents a problem for which there is no elegant solution, and the best solution available is to deorbit Pluto and return closer to Earth until data rates are sufficient. Data rate estimates for Pluto, Saturn, and Jupiter distances are shown in Table 6.15.

Table 6.15: Data Rates During Return to Earth

	<b>Data Rate</b>	<b>Time to Return 1 TB</b>
<b>Pluto</b>	10,000 bits/sec	25 years
<b>Saturn</b>	190,000 bits/sec	487 days
<b>Jupiter</b>	700,000 bits/sec	132 days

## 6.7 Thermal Control

The thermal control system of the Persephone mission will closely resemble that of New Horizon's. In both cases, the main goal of the system is to keep all components of the spacecraft at safe operating temperatures-most importantly the scientific payloads. Each component has different operating temperatures and sensitivities to changes in temperature such as expansion, contraction, inefficiency, and more. To avoid this, the bulk spacecraft temperature must be kept between 10 and 30 degrees Celsius; this is a challenge as the estimated temperature of a metal sphere in orbit around Pluto is -230 degrees Celsius and 6 degrees Celsius while in Earth orbit. Since neither temperature is within the optimal range, several systems and components will be required to keep the temperature within the operational range. However, the Persephone mission will be using two RTGs to power the spacecraft which gives off large amounts of excess heat, so it is important to also make sure heat can exit the system as well as keep the spacecraft at optimal temperatures. These components fall into two different categories: active and passive thermal control.

### 6.7.1 Passive Thermal Control

The chief passive thermal control method in place on the spacecraft will be the Multi-Layer Insulation (MLI) that covers the entire structure and acts essentially as a thermos for the spacecraft. This layering consists of Kapton on the surface with albedo values ranging from 0.95 to 0.99 given different wavelengths of light to reject almost all incoming solar radiation. The middle layers of the MLI are composed of 18 layers of Dacron with small vacuum pockets to limit conduction through the MLI. The interior portion of the MLI is made up of Mylar to keep the most possible heat within the spacecraft and not lose any heat to radiation.

Other passive methods include all forms of radiators; these will be some of the few parts on the outside of the spacecraft that are exposed other than the MLI. These radiators will be strategically placed near components producing excess heat or with a low thermal operating range. To remove all heat provided by the RTG, it is estimated three 0.5 meter squared radiator plates will be enough to manage the heat rejection needed. These will only radiate heat when the heat pipes deliver the extra heat to the

radiator plates. The RTG will need several radiators to allow the excess heat to escape as its contents decomposes, as will any high wattage instrument such as the thermal camera. Another important passive system will be the constant conductance heat pipes (CCHPs) throughout the spacecraft, which allow for continuous heat transfer to maintain total thermal control. These heat pipes will also be responsible for heating the fuel tanks of Iodine and Hydrazine by running around the surface of the fuel tanks. The hydrazine fuel tank will be kept as close to 21 degrees Celsius, which at the calculated pressures for the tank, is the optimal temperature. This temperature falls between the optimal spacecraft bulk temperature range, so it will be heated similarly to the rest of the spacecraft. The Iodine is only to be heated when necessary, so the piping transferring the Iodine to the thrusters will be heated by an external heat pipe. Conduction from the pipes to the aluminum tanks will then heat the most thermally sensitive portions of the heat tank being the outermost portions of the fuel. This can be accomplished by the heat pipes due to the fact the loss of heat only due to minor radiation and conduction through the supports[4]site

### 6.7.2 Active Thermal Control

Active thermal control systems are connected to a computer that is separately powered and operated from Persephones main computer in order to ensure the thermal operations remain nominal in the case of other failures. This computer has both low weight and wattage so it does not significantly impact other operations of the spacecraft. The purpose of this computer is to control all the louvers, shunts, and heaters as well as to receive input from thermal sensors around the craft. The louvers act similarly to the radiators mentioned above but can be opened and closed to radiate more or less heat depending on the thermal requirements of the spacecraft at any given time. Open louvers radiate about six times more heat than when closed. These are placed near all scientific instruments to be opened when the instrument is on and generating more heat than is necessary to keep the temperature in operational range. Shunts are simply resistors that will turn any excess electrical energy provided by the RTG into heat. This heat is then moved to either a radiator or open louver to be radiated into space or moved to another part of the craft in need of heating via constant conductance heat tubing.

### 6.7.3 Descent Probes Thermal Control

The descent probes are located on the exterior of the main body of the spacecraft making thermal control a larger challenge and will also separate from the ship, so the descent probes must be able to heat independently. While en route to Pluto, the descent probes will be stored on the outside of the craft equidistant from one another. These storage units will be covered by MLI layering to retain the heat generated within. Each descent probe will be placed near a 5 Watt heater powered by an umbilical to the main spacecraft; this umbilical powers all three connected storage units and will also charge the batteries on the descent probes prior to release. To limit the risk of thermal exposure there will only be one point of egress for power to the descent probes from the main spacecraft. Once separated, the descent probes will be thermally independent by powering an internal heating resistor using power from the charged battery. Given the short transit time to impact, this will be sufficient to ensure the thermal safety of each of the descent probes.

## 6.8 Guidance, Navigation, and Control

### 6.8.1 Overview

Momentum management on the spacecraft is critical to the mission success as the spacecraft must maintain adequate control authority for long-duration electric propulsion thrusting and accurate scientific observations. Experience from previous deep-space missions with an electric primary propulsion system such as Deep Space 1 (DS1) and Dawn have shown that this momentum management is not as trivial as it may seem [25]. Throughout engine operation, a small parasitic torque is generated around the thrust direction. This torque is often referred to as "swirl torque" and must be constantly accounted for while the electric propulsion system is thrusting. Thus, an attitude control system that can operate almost constantly is required.

DS1 and Dawn used different attitude control systems to handle this problem. DS1 used a hydrazine reaction control system (RCS) as the primary attitude control system; however, when the star tracker famously failed during the extended mission, the spacecraft was significantly limited by the hydrazine propellant it had to perform all additional maneuvers. The Dawn spacecraft addressed this



potential issue by incorporating a reaction wheel assembly (RWA) into the design. The advantage of using a RWA coupled with a RCS is the ability to use the reaction wheels to constantly correct for the swirl torque while thrusting and only using the RCS to desaturate the wheels. This allows for the conservation of the expendable fuel at the expense of added mass and power requirements of the RWA. Despite incorporating this improved system, the Dawn spacecraft has not gone without its own attitude control issues. In 2017, the spacecraft lost the third of its four reaction wheels, leaving it operating with only one [26]. Thanks to its hydrazine thrusters, it was able to continue its mission without much of an impact, but it is clear that even using a dually-redundant system is not infallible.

### 6.8.2 Disturbance Torques

The requirements of the attitude control system are dictated by the disturbance torques it experiences over the mission life. These disturbance torques vary in magnitude over the mission, and a clear understanding of how these torques affect the spacecraft at each point in the mission is critical to an accurate attitude control system design. For this particular mission, the disturbance torques experienced come from the gravity gradient experienced while orbiting Pluto, solar radiation pressure, the magnetic field of Jupiter during flyby, and the electric propulsion swirl generated by the electric propulsion system. The maximum torques experienced are shown in Table 6.16.

Table 6.16: Maximum Disturbance Torques

<b>Gravity Gradient</b>	$0.483 \times 10^{-6} Nm$
<b>Solar Radiation</b>	$1.788 \times 10^{-6} Nm$
<b>Magnetic</b>	$0.133 \times 10^{-6} Nm$
<b>Electric Propulsion Swirl</b>	$27.839 \times 10^{-6} Nm$

Analyzing the transient effects of these disturbance torques over the mission duration, shown in Figure 6.25, it is clear that different torques act as the primary disturbance throughout the mission. Early on, solar radiation pressure serves as the primary disturbance. However, as the spacecraft moves deeper into the solar system this force becomes significantly reduced. Once the electric propulsion system begins functioning, the swirl torque generated becomes a significant disturbance. This torque is the largest

experience throughout the spacecraft mission. After arrival to the Pluto system, the gravity gradient torque becomes the primary disturbance force, with intermittent swirl torque as the electric propulsion system is used to change its orbit.

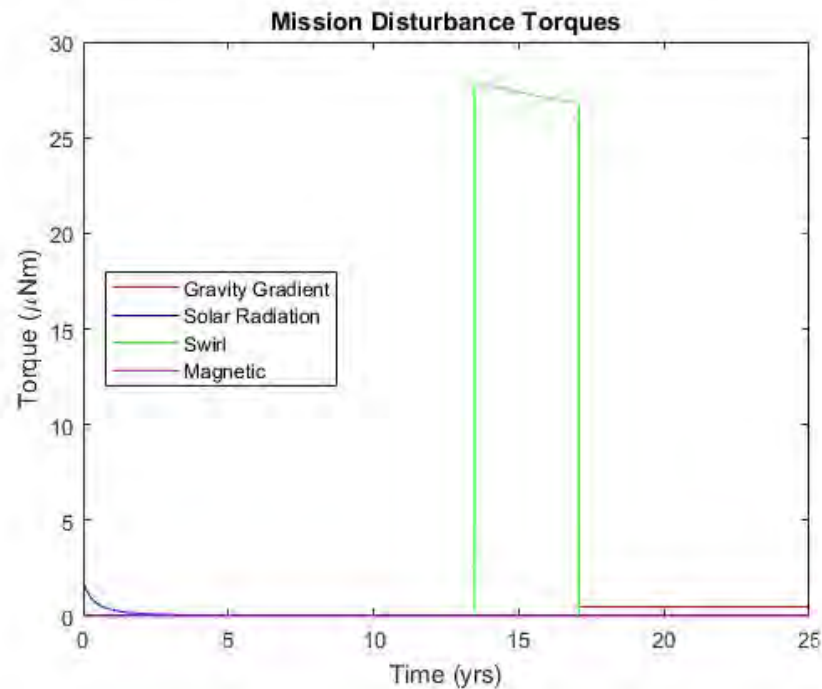


Figure 6.25: Mission Disturbance Torque Breakdown

### 6.8.3 System Selection

Persephone will follow in Dawn's footsteps and use a dual RWA and RCS system; however, due to the long-duration nature of this mission, highly reliable reaction wheels must be used to avoid excessive use of its limited propellant. With an interplanetary cruise phase of over 17 years before arriving at Pluto with 3.6 years of near-constant electric propulsion thrusting, maintaining control with the RWA is crucial to minimize the propellant use.

RWA's primary failure occurs from the mechanical bearings wearing out over time. Given that reaction wheels rotate at thousands of RPM over years of service, friction in the bearings can wear down the wheel. This wear results in particulates which can become embedded into the lubricant and accelerate the

wear process even more. This issue is typically handled by properly lubricating the bearings to prevent this initial wear; however, there are often issues with lubricant distribution, especially at low rotational speeds.

A relatively recent solution to this wear problem has been the increased development of magnetic-bearing RWAs. These designs avoid the root cause of the problem completely by removing the physical contact between the bearing and the reaction wheel, providing a more reliable system that is much less susceptible to mechanical failure. To check the validity of this technology compared to its mechanical equivalent, a trade study is conducted using the angular momentum of the devices as a baseline for comparison.

Table 6.17: Mechanical vs. Magnetic Bearing Reaction Wheels

	<b>Mechanical</b>	<b>Magnetic</b>
<b>Reaction Wheel</b>	Rockwell Collins RSI 25 [27]	Rockwell Collins MWI 30-400/37 [28]
<b>Angular Momentum</b>	25 <i>Nms</i>	30 <i>Nms</i>
<b>Torque</b>	0.220 <i>Nm</i>	0.400 <i>Nm</i>
<b>Mass</b>	7.15 <i>kg</i>	15.3 <i>kg</i>
<b>Nominal Power</b>	5 <i>W</i>	20 <i>W</i>
<b>Power at Mass Torque</b>	50 <i>W</i>	300 <i>W</i>

From this analysis, there are many key conclusions that can be drawn. For an approximately equivalent angular momentum, the magnetic bearing RWA is able to perform any given maneuver twice as quickly as the mechanical bearing RWA, but this increased ability comes at a significant cost. The magnetic bearing RWA requires an immense amount of power input for both nominal and peak operation and has twice as much mass as its mechanical counterpart. While the robustness and increased reliability is a significant draw, the strict mass requirements of the spacecraft coupled with the limited power available dictate that a mechanical RWA be used. To address the reliability of the RWA over the primary mission life, high quality reaction wheels with robust testing must be selected for the mission. While this comes at the expense of increased mission cost, the impact on mission success of the reaction wheel failure is too large to be glossed over.

Momentum management of the spacecraft over the mission is critical to preventing reaction wheel

failure. As momentum builds in the reaction wheels as they counter the disturbance torques, the wheels must be desaturated to prevent failure. Using a 1.3 factor of safety, the momentum accumulation and RWA desaturation required is shown in Figure 6.26.

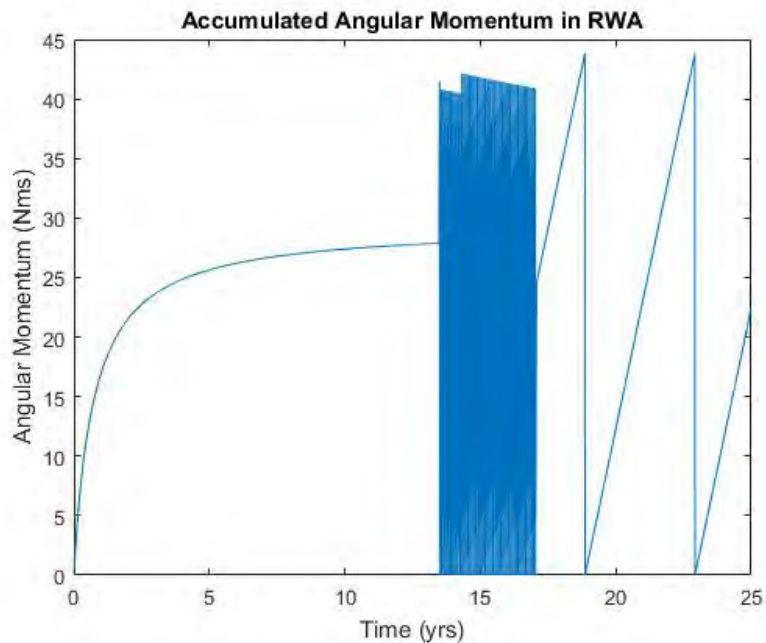


Figure 6.26: Momentum Dumping during Mission

This analysis provides a significant over-simplification of the design as it does not account for torques about different axes and assumes only one wheel is accumulating the momentum. This allows for a very conservative design of the GN&C system. Given the disturbance torques experienced, the RWA must be unloaded 53 times over the baseline course of the mission. This momentum dumping is provided by the RCS. During the electric propulsion thrusting phase where momentum is accumulated the most rapidly, the RWA must be dumped every 25 days.

The RCS used to desaturate will operate using hydrazine monopropellant. A tank containing 25 kg of hydrazine will be used for the 25 year primary mission. This propellant, coupled with the ability to desaturate the RWA in two degrees of freedom using the electric propulsion system will be sufficient. The hydrazine tank design is optimized similar to the propellant tank and the design is detailed in Table 6.18.

The same optimization weights from Table 6.10 are used.

Table 6.18: Hydrazine Tank Design

Storage Temperature ( $^{\circ}C$ )	21
Storage Pressure ( $psi$ )	44.1
Tank Radius ( $m$ )	0.181
Tank Thickness ( $mm$ )	0.060
Tank Mass ( $kg$ )	0.069

## 6.9 Attitude Determination

Attitude determination is crucial to the success of the Persephone mission for two primary reasons. First, accurate attitude information is needed at all times for proper navigation while using electric propulsion. Without accurate methods of attitude determination, errors will accrue, and the spacecraft will very quickly diverge from its intended course. Second, accurate attitude information is essential to gathering precise scientific data and sending it back to Earth. As this mission's primary goal is to gather and send data about the Pluto-Charon system, it is critical that the spacecraft be able to reliably conduct scientific observations and report the results back to Earth.

The attitude determination systems for the spacecraft are heritage from New Horizons and updated to the present norms. While other systems were investigated, concerns of system mass, power requirements, and reliability indicated that heritage technology should be used. The primary method of attitude determination will be two star trackers mounted on the spacecraft. Ball Aerospace's CT-2020 star tracker has been selected for this mission due to its low mass, low power requirements, and high performance. Used together, the two star trackers provide  $<1.0$  arc-second accuracy for the mission. Given that the pointing requirement for the high-gain antenna is about 0.2 degrees for Earth communication, these are sufficient for the primary attitude determination method. A diagram of the system can be seen in Figure 6.27.

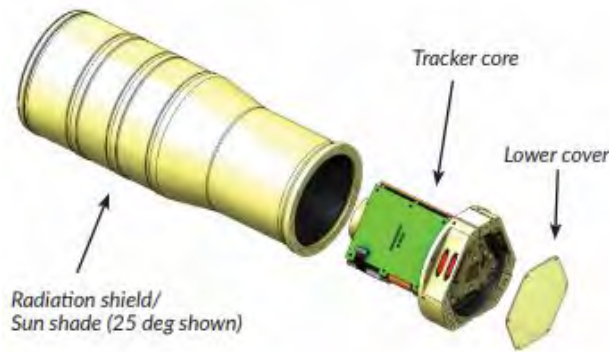


Figure 6.27: Ball Aerospace CT-2020 Star Tracker [29]

Persephone will use two Adcole Fine Sun Sensors that are installed orthogonally to each other so that the sun vector can be determined. This equipment is directly heritage from the New Horizons mission and is proven to be an effective redundant system.

An inertial measurement unit (IMU) provides a third redundant method for attitude determination. While this system provides additional reliability of the overall attitude determination subsystem, there are concerns about its viability for the entire primary mission. The main issues with relying on an IMU are twofold. First, there are concerns of the attitude drift over time. Because IMUs use accelerometers and gyroscopes to measure the translational and rotational changes, respectively, in spacecraft acceleration and then integrate backwards to determine position, there is always concern in the accuracy of the system over time. Generally the accumulated drift can be corrected over time via inputs from the other attitude determination systems and is thus not a significant hindrance; however, if there are system failures in the other two methods, then the accuracy of the spacecraft attitude determination is severely limited by the IMU.



Figure 6.28: Adcole Fine Sun Sensor (*courtesy Adcole Corporation*)

The second concern for utilizing an IMU is the system reliability. Because the system requires gyroscopes, mechanical failure of one or more is of significant concern. Typical spacecraft systems follow a "bathtub" curve, shown in Figure 6.29, which includes high failure rates at both BOL and EOL. This holds especially true for constantly moving components such as gyroscopes. By the end of the 25 year primary mission, there is a high probability that there will have been a failure in this system. Alternatives such as a laser-ring gyroscope provide exciting and new solutions to this problem that were unavailable to New Horizons; however, due to the power constraints on the spacecraft, this system is not feasible.

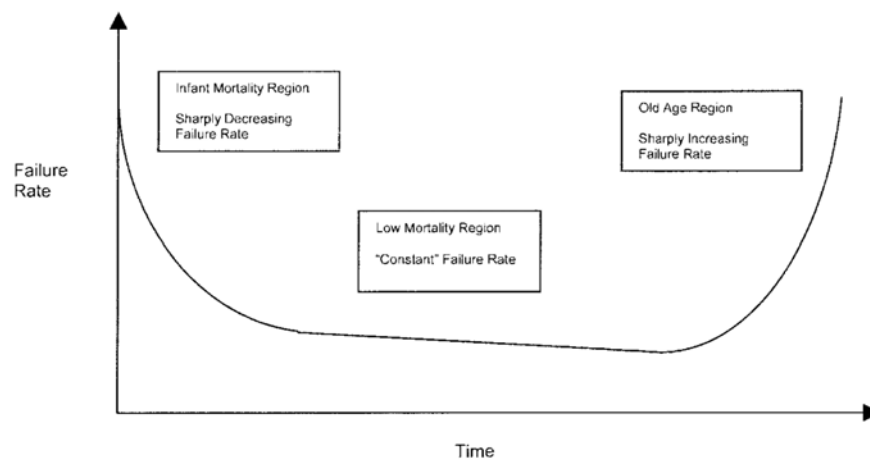


Figure 6.29: Bathtub Reliability Curve[30]

## 7 Cost Evaluation

Mission costs are analyzed over a 25 year period using the Large Satellite Cost Model for spacecraft system development and production, Mission Operations Cost Estimating Tool (MOCET) for operations, and the DSN Aperture Fee Calculator for DSN usage [31][32]. A summary of the costs is included in Table 7.1.

Table 7.1: Mission Cost Analysis

<b>Subsystem</b>	<b>Cost (FY17\$K)</b>	<b>Res Cost (FY17\$K)</b>
Launch on SLS	853,000	85,300
Scientific Instruments	102,350	10,235
Bus	191,718	28,758
Comms	21,311	4,337
Power	15,675	4,703
Thermal	5,625	562
Att. Det.	13,824	1,382
ACS	8,542	854
TT&C	5,434	1,630
DSN Usage	151,349	15,035
Ops	792,636	118,895
<b>Sums</b>	<b>2,160,464</b>	<b>271,692</b>
<b>Total Cost</b>		<b>2,432,156</b>

The cost of this mission puts Persephone deep into the Large Strategic Science Missions class. This class of mission typically experiences cost overruns, so while cost overruns have already been factored into the mission cost presented in 7.1, it is safe to assume that these costs will be exceeded at least marginally.



## 8 Mission Summary & Conclusions

The Persephone spacecraft enables further exploration of the Pluto system with an orbital-class mission around the dwarf planet. Using a low-power, electric, multiple fault-tolerant propulsion system, spacecraft mass can be minimized while still achieving the mission goals. Internal power generation through two GHPs-RTGs provide the spacecraft with constant power and enables it to operate through its entire 25 year primary mission lifetime. Using a large high-gain antenna, critical data can be sent back to Earth at a low data rate before the spacecraft begins its deorbit phase to return the rest of the stored data.

Using the SLS Block 1B cargo variant, Persephone can be launched with a high C3 energy, enabling it to complete its interplanetary trajectory quickly while minimizing the constraints placed on the propulsion system. With the help of a Jupiter gravity assist, the spacecraft is able to reach Pluto after 17 years, including a 3.6 year deceleration phase. Upon Pluto Orbital Insertion, the spacecraft has approximately 8 years to conduct scientific observations before it must deorbit the system and head back to the inner solar system.

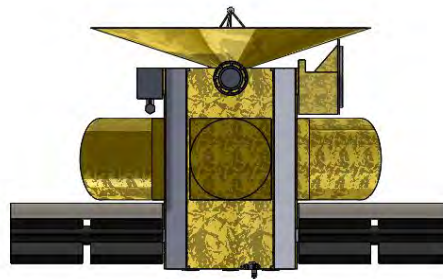


Figure 8.1: Persephone Spacecraft

Table 8.1: Mission Timeline

Event	Date
Earth Launch	07 Jan 2030
JGA	30 Jun 2031
Deceleration Start	27 Jun 2043
POI	06 Feb 2047
Pluto Deorbit	07 Jan 2050

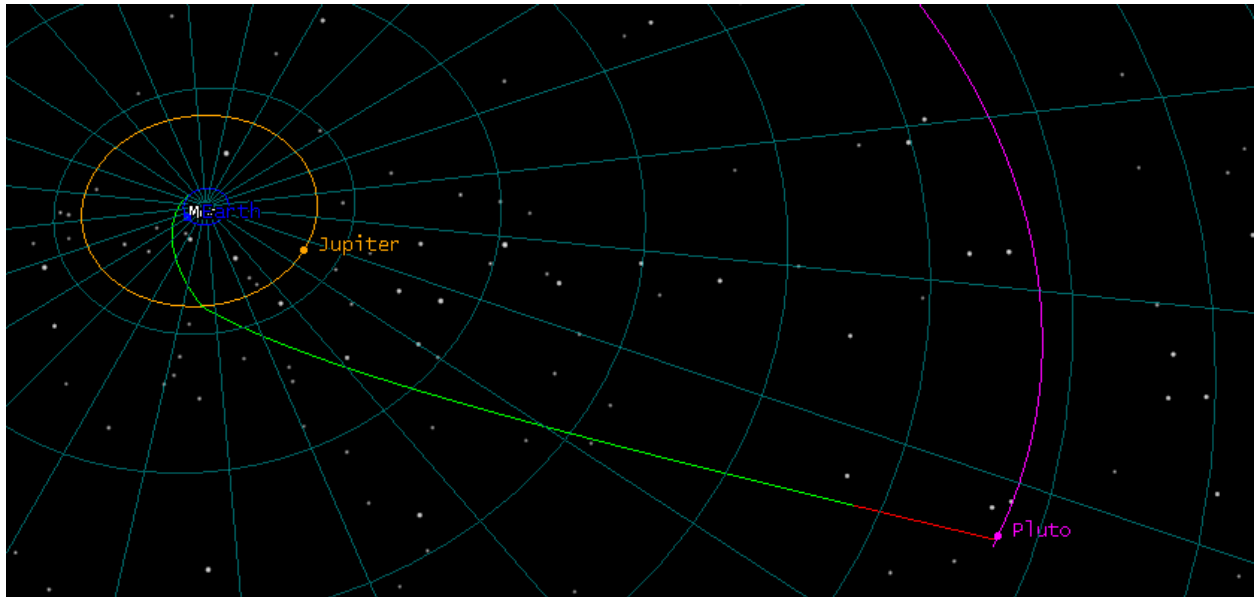


Figure 8.2: Interplanetary Trajectory

Once in orbit around the system, detailed scientific observations are enabled via a unique combination of improved New Horizons heritage instruments, improved Cassini inherited instruments, and innovative descent probes. These tools enable the scientific community to make groundbreaking discoveries regarding Pluto's atmosphere, geology, history, and interactions with its satellites. Complete mapping of all celestial bodies with the system will be accomplished—including Styx, Nix, Kerberos, and Hydra.

As an orbital mission, Persephone will enable discoveries of the Pluto system that shed light on the history of the solar system and the mysterious objects that lie in the Kuiper Belt. For a world left cold and forgotten naught for a postage stamp and a few disgruntled engineers, Pluto serves as an example of the mystery and diversity embedded into the fabric of our solar system, eagerly awaiting those brave souls who dare to question it.

## Acknowledgements

The entire Persephone design team would like to extend our deepest gratitude to the many people who supported and advised the team. Special thanks goes to Dr. Dale Chimenti for the technical reviews and guidance throughout the design process. A huge thank you to Dr. Massimo Marengo for his time in the early stages of the design project, as he provided much-needed insight into the scientific interests of the Pluto system and guided us to many great sources. An invaluable resource, the team would like to thank Dr. Rostislov Spektor taking the time to meet during his brief visit to Iowa State University. His feedback on the electric propulsion system and the complexities of the problem led the team to make many major design improvements and design a much more effective spacecraft. We'd like to thank Dr. Travis Sippel for taking some time to discuss the spacecraft design - particularly the thermal control system. Last but not least, our gratitude goes out to Dr. Denise Podolski for the communications system advisement. Her expertise in spacecraft communications was extremely beneficial given the extreme burden that this system takes for a Pluto mission.

## References

- [1] R. J. Terrile R. Staehle and S. S. Weinstein. “To Pluto by Way of a Postage Stamp”. In: *Planetary Report* (Sept. 1994), pp. 4–11.
- [2] Y. Guo and R. W. Farquhar. “New Horizons Mission Design”. In: *Space Sci Rev* 140 (2008), pp. 49–74.
- [3] J. M. Moore et al. “The geology of Pluto and Charon through the eyes of New Horizons”. In: *Science* 351.6279 (2016), pp. 1284–1293.
- [4] G. R. Gladstone et al. “The atmosphere of Pluto as observed by New Horizons”. In: *Science* 351.6279 (2016), p. 1284.
- [5] W. M. Grundy et al. “The formation of Charon’s red poles from seasonally cold-trapped volatiles”. In: *Nature* 539 (2016), pp. 65–68.
- [6] H. A. Weaver et al. “The small satellites of Pluto as observed by New Horizons”. In: *Science* 351.6279 (2016), p. 1284.
- [7] National Aeronautics and Space Administration. *Systems Engineering Handbook, Rev 1*. Tech. rep. Hannover, MD: NASA Center for AeroSpace Information, 2007.
- [8] NASA Office of Planetary Protection. *Planetary Protection Provisions for Robotic Extraterrestrial Missions*. Tech. rep. NASA, 2011.
- [9] ESA Science & Technology. *Instruments*. Feb. 2005. URL: [sci.esa.int/cassini-huygens/34954-instruments/?fbodylongid=1623](http://sci.esa.int/cassini-huygens/34954-instruments/?fbodylongid=1623).
- [10] NASA JPL. *RSS*. Jan. 2017. URL: <https://saturn.jpl.nasa.gov/radio-science-subsystem/>.
- [11] McComas et al. *Solar Wind Around Pluto (SWAP) Instrument Aboard New Horizons*. Southwest Research Institute. 2016. URL: <https://arxiv.org/ftp/arxiv/papers/0709/0709.4505.pdf>.
- [12] *Instrument Overview - New Horizons*. Spaceflight 101. 2018. URL: [spaceflight101.com/newhorizons/instrument-overview/](http://spaceflight101.com/newhorizons/instrument-overview/).
- [13] *Trajectory Optimization Tool v2.1*. Orbit Hanger Mods. Apr. 2012. URL: <https://www.orbithangar.com/searchid.php?ID=5418>.
- [14] National Aeronautics and Space Administration. *Space Launch System (SLS) Mission Planner’s Guide*. Tech. rep. NASA, 2017.
- [15] *B-Plane Targeting*. Satellite Tool Kit. Apr. 2018. URL: <http://help.agi.com/stk/index.htm#gator/eq-bplane.htm>.
- [16] M.G. Kivelson K.K Khurana et al. “The configuration of Jupiter’s magnetosphere”. In: *Bagenal, F.; Dowling, T.E.; McKinnon, W.B. Jupiter: The Planet, Satellites and Magnetosphere* (2004).

- [17] C.T. Russell. “Planetary Magnetosphere”. In: *Reports on Progress in Physics* 56.6 (1993), p. 687.
- [18] G. P. Sutton and O. Biblarz. *Rocket Propulsion Elements*. 7th ed. John Wiley & Sons, 2001.
- [19] *NASA’s Juno Spacecraft Breaks Solar Power Distance Record*. NASA. Jan. 2016. URL: <https://www.jpl.nasa.gov/news/news.php?feature=4818>.
- [20] T. Haag H. Kamhawi et al. “Overview of Iodine Propellant Hall Thruster Development Activities at NASA Glenn Research Center”. In: American Institute of Aeronautics and Astronautics. Salt Lake City, UT, 2017.
- [21] B. Pote J. Szabo et al. “High Throughput 600 Watt Hall Effect Thruster for Space Exploration”. In: *American Institute of Aeronautics and Astronautics* (2017).
- [22] *Mission Critical On-Orbit Data Management for High-Reliability Applications*. Southwest Research Institute. URL: <https://www.swri.org/solid-state-recorders>.
- [23] R. K. Nimmagadda. *A Highly Reliable Non-Volatile File System for Small Satellites*. Tech. rep. University of Kentucky, 2008.
- [24] Integral Memory. *Smartphone and Tablet microSDHC/XC UHS-I U1 Card*. 2018. URL: [https://www.integralmemory.com/sites/default/files/products/specifications/Integral\\_Smartphone\\_and\\_Tablet\\_microSDHC-microSDXC\\_spec\\_sheet\\_0.pdf](https://www.integralmemory.com/sites/default/files/products/specifications/Integral_Smartphone_and_Tablet_microSDHC-microSDXC_spec_sheet_0.pdf).
- [25] C. A. Vanelli B. A. Smith and E. R. Swenka. “Managing Momentum on the Dawn Low Thrust Mission”. In: *IEEE* (2009).
- [26] *Dawn Observing Ceres; 3rd Reaction Wheel Malfunctions*. NASA. Apr. 2017. URL: <https://www.nasa.gov/feature/jpl/dawn-observing-ceres-3rd-reaction-wheel-malfunctions>.
- [27] Rockwell Collins. *High Motor Torque Momentum and Reaction Wheels*. 2018. URL: <https://www.rockwellcollins.com/Products-and-Services/Defense/Platforms/Space/High-Motor-Torque-Momentum-and-Reaction-Wheels.aspx>.
- [28] Rockwell Collins. *MWI Magnetic Bearing Momentum and Reaction Wheels with Internal Wheel Drive Electronics*. 2007. URL: [http://www.electronicnote.com/RCG/MWI\\_A4.pdf](http://www.electronicnote.com/RCG/MWI_A4.pdf).
- [29] Ball Aerospace. *CT-2020 Fact Sheet*. Jan. 2018. URL: [http://www.ball.com/aerospace/Aerospace/media/Aerospace/Downloads/D3408\\_CT2020\\_0118.pdf?ext=.pdf](http://www.ball.com/aerospace/Aerospace/media/Aerospace/Downloads/D3408_CT2020_0118.pdf?ext=.pdf).
- [30] M. D. Griffen and J. R. French. *Space Vehicle Design*. Ed. by J. A. Schetz. 2nd ed. American Institute of Aeronautics and Astronautics, Inc., 2004.
- [31] J. Keesee D. W. Miller and C. Jilla. *Space Systems Cost Modeling*. Tech. rep. Massachusetts Institute of Technology, 2003.
- [32] K. Brancato B. Fox and B. Alkire. *Guidelines and Metrics for Assessing Space System Cost Estimates*. Tech. rep. RAND Corporation, 2008.

- [33] E. Wright. *Doppler Shift*. University of California, Los Angeles. Feb. 2002. URL:  
<http://www.astro.ucla.edu/~wright/doppler.htm>.
- [34] *New Horizons Thermal Control System*. Matt Bergman. Aug. 2015. URL:  
<https://mattcbergman.com/2015/08/02/new-horizons-thermal-control-system>.